

The mid- and far-infrared colours of AGB and post-AGB stars*

M.A.T. Groenewegen

Instituut voor Sterrenkunde, Katholieke Universiteit Leuven, Celestijnenlaan 200B, B-3001 Leuven, Belgium

received, accepted: 27 October 2005

Abstract. With the advent of space missions, like SPITZER and ASTRO-F, with sensitive detectors in the near- and mid-infrared covering a reasonable field-of-view and having a good spatial resolution, it will be possible to detect individual AGB stars in Local Group galaxies. The filters used by these missions are non-standard and different from mission to mission. In this paper, the colours of mass-losing AGB and post-AGB stars are calculated in the broad-band filters of the SPITZER and ASTRO-F missions, as well as Bessell *V, I* and 2MASS *J, H, K* to connect these results to existing ground-based data. The models are calculated for carbon- and oxygen-rich chemistry and cover different effective temperatures and dust compositions.

Key words. circumstellar matter – stars: mass loss – stars: AGB and post-AGB – Radiative transfer

1. Introduction

Asymptotic Giant Branch (AGB) and post-AGB stars are prominent emitters in the infrared (IR), firstly because of their low effective temperatures and secondly because of their mass loss rates, which can go up to $10^{-4} M_{\odot} \text{yr}^{-1}$ for brief spells of time, in conjunction with dust formation. The importance of the mid-IR was first demonstrated by the results of the IRAS mission (Beichman et al. 1988) which discovered many mass-losing AGB stars (e.g. van de Veen & Habing 1988) in the solar neighbourhood but also luminous mass-losing AGB stars in the Large Magellanic Cloud (LMC) (see Reid et al. 1990, Reid 1991, Wood et al. 1992, Zijlstra et al. 1996, Loup et al. 1997), and Small MC (Whitelock et al. 1989, Groenewegen & Blommaert 1998), at the limiting magnitudes of IRAS near 100 mJy at 12 micron. When the ISO satellite was launched many of these mass-losing AGB stars discovered by IRAS in the MCs were followed up (e.g. Trams et al. 1999, van Loon et al. 1999), and new surveys in the MCs were conducted (Loup et al. 1999a, b), in particular using the ISOCAM instrument (Cesarsky et al. 1996, Blommaert et al. 2003) that had imaging filters covering 3 to 15 micron with a field-of-view of typically $1.5'$ by $1.5'$. In addition, the Galactic Centre region, where IRAS was severely confusion limited, was imaged during the ISOGAL survey (Omont et al. 2003), discovering many AGB stars (Omont et al. 1999).

IRAS and ISO showed the importance of the IR region, from the Near-IR to the Far-IR. The SPITZER mission (Werner et al. 2004), launched on 25 August 2003, and the ASTRO-F mission (e.g. Pearson et al. 2004, Matsuhara et al. 2005), with a planned launch date of spring 2006, carry a range of imaging

filters that cover the near-, mid- and far-IR. Due to an improved sensitivity and spatial resolution it is expected to resolve individual AGB stars in galaxies far beyond the MCs.

In the present work, series of dust radiative transfer models are presented that cover the spectral types, dust composition and mass loss rates seen for Galactic AGB stars. The flux-densities are computed in the SPITZER IRAC (Fazio et al. 2004) and MIPS (Rieke et al. 2004) filters, and the ASTRO-F IRC, MIR-S, MIR-L and FIS filters. For comparison to ground based data *V, I* and *J, H, K* magnitudes are also presented.

Sect. 2 presents the radiative transfer model and the inputs to it, including the various dust compositions considered. Sect. 3 gives details on the considered filter curves and the adopted flux-calibration. Sect. 4 presents the results, scaling laws to arbitrary luminosities and distances, and some caveats in the use of the results. Sect. 5 concludes by illustrating colour-magnitude diagrams for AGB stars in M31 and the Wolf-Lundmark-Melotte (WLM) galaxy.

Earlier results from this kind of dust modelling (in particular for the ISOCAM filters) were available as private communication and have been used in Blommaert et al. (2000), Ortiz et al. (2002) and Ojha et al. (2003).

2. Inputs to the Radiative Transfer model

The models have been calculated with a 1-dimensional dust radiative transfer (RT) code that solves the radiative transfer equation and the thermal balance equation in a self-consistent way (Groenewegen 1993, also see Groenewegen 1995).

Basic inputs to the model are the stellar luminosity (*L*), distance (*d*), photospheric spectrum, (total) mass loss rate, dust-to-gas ratio, (terminal) outflow velocity, dust condensation temperature (*T_c*) and composition of the dust.

Send offprint requests to: Martin Groenewegen
(groen@ster.kuleuven.be)

* Appendix A is available in the on-line edition of A&A.

The models have been calculated for (arbitrary) values of $L = 3000 L_{\odot}$, $d = 8.5$ kpc, $v_{\infty} = 10$ km s $^{-1}$, dust-to-gas (Ψ) ratio = 0.005, and no interstellar reddening. Scaling relations will be presented later.

Photospheric input spectrum for O-rich stars are taken from Fluks et al. (1994) for spectral types M0 ($T_{\text{eff}} = 3850$ K), M6 ($T_{\text{eff}} = 3297$ K) and M10 ($T_{\text{eff}} = 2500$ K). For C-rich stars the models by Loidl et al. (2001) for $T_{\text{eff}} = 3600$ and 2650 K are considered¹.

Several types of dust are considered that cover the main features observed in AGB stars. The absorption coefficients as a function of wavelength are displayed in Figure 1. For dust around O-rich stars they are:

- 100% Aluminium Oxide (AlOx; amorphous porous Al₂O₃), with optical constants from Begemann et al. (1997) and assuming a condensation temperature of $T_c = 1500$ K.
- A combination of 60% AlOx and 40% Silicate (optical constants from David & Pegourie 1995) and assuming a condensation temperature of $T_c = 1500$ K.

The dust species with 60 to 100% AlOx can explain the observed Spectral Energy Distributions (SEDs) and ISOCAM CVF 5-14 μm spectra in Galactic Bulge AGB stars which have mass loss rates up to $10^{-7} M_{\odot} \text{yr}^{-1}$ (Blommaert 2003, Blommaert et al. 2005, in preparation).

- 100% silicate with $T_c = 1000$ K.

For dust around C-rich stars two species are considered:

- A combination of 85% Amorphous Carbon (AMC) and 15% Silicon Carbide (SiC) with optical constants from, respectively, Rouleau & Martin (1991) for the AC1 species and α -SiC from Pégourié (1988). A T_c of 1200 K is adopted.
- 100% AMC with a T_c of 1000 K.

This range of AMC with zero to 15% percent SiC and the corresponding condensation temperatures can explain the SEDs and IRAS LRS spectra of the majority of (Galactic) C-stars (Groenewegen 1995, Groenewegen et al. 1998). For all dust species a uniform grain size of $0.1 \mu\text{m}$ is adopted.

3. Flux Calibration

In this paper the broad-band filters of the SPITZER and ASTRO-F missions are considered. Both contain filters in the near- and mid-IR which are ideal to identify mass losing stars. Filtercurves have been obtained from official websites², and are reproduced in Fig. 2. The filter names and their central wavelengths are given in Table 1.

To connect this data to existing ground-based data Bessell V , I and 2MASS J , H , K magnitudes are also calculated, whose filter curves are also shown in Fig. 2.

¹ And with a C/O ratio of 1.1.

² http://ssc.spitzer.caltech.edu/mips/spectral_response.html;
http://ssc.spitzer.caltech.edu/irac/spectral_response.html;
<http://www.ir.isas.jaxa.jp/ASTRO-F/Observation/>

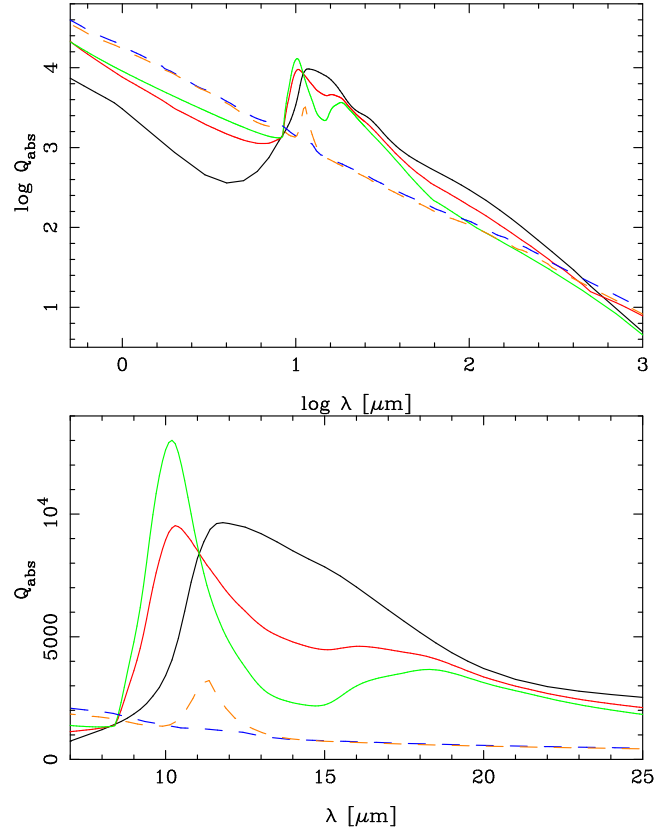


Fig. 1. The absorption efficiency for the five dust species considered here, plotted over the whole wavelength range (top panel), and the mid-IR. Dashed lines indicate 100% AMC, and the combination of 85% AMC + 15% SiC, which peaks near $11.3 \mu\text{m}$. The solid lines indicate 100% silicate (with a narrow feature that peaks near $10 \mu\text{m}$), 40% silicate + 60% AlOx, and 100% AlOx (with a broad feature that peaks near $12 \mu\text{m}$).

The main output of the RT code is the flux emerging from the AGB star and its dust envelope. This flux is folded with the filter curves and flux-densities and magnitudes are calculated from (following the definition used by IRAS, ISOCAM and IRAC, see e.g. Blommaert et al 2003):

$$m_{\lambda} = -2.5 \log \left(\frac{\int (\lambda/\lambda_0) F_{\lambda} R_{\lambda} d\lambda}{\int R_{\lambda} d\lambda} \right) + m_0 \quad (1)$$

The zero-points, m_0 , are calculated from a reference spectrum for Vega calculated using the MARCS code (Decin, private communication). The resulting and adopted flux-densities for a zero-magnitude star are listed in Table 1.

4. Results for AGB and post-AGB stars

As mentioned before, the results of the numerical code have already been used to successfully fit the SEDs of individual stars (Groenewegen 1994a,b, 1995, 1997; Groenewegen et al. 1995, 1997, 1998) and predict the colours of AGB stars (Blommaert et al. 2000, Ortiz et al. 2002, Ojha et al. 2003) and has been bench-marked against other codes (Ivezic et al. 1997). To illustrate the typical accuracies that can be achieved in fitting SEDs

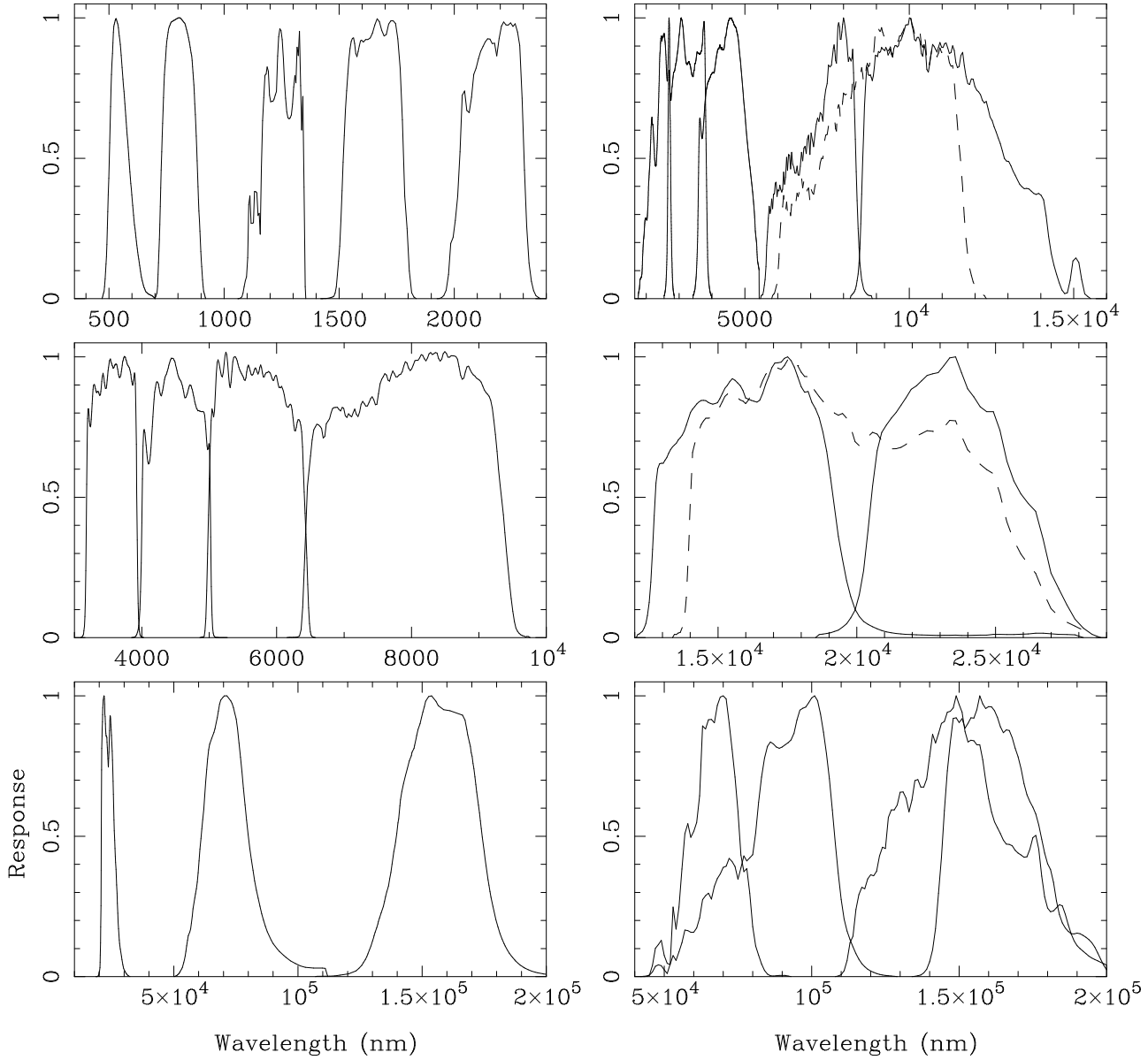


Fig. 2. Filter curves adopted: Bessell *VI, 2MASSJHK* (left top), Spitzer-IRAC (left middle), Spitzer-MIPS (left bottom), ASTRO-F IRC and MIR-S (right top), ASTRO-F MIR-L (right middle), and ASTRO-F FIS (right bottom).

and colours, Figure 3 shows a fit to the SED and the IRAS LRS spectrum of the Mira V Oph (cf. Figure 33 in Groenewegen et al. 1998), but now with the 2650 K model atmosphere instead of a black-body in Groenewegen et al. (1998). The agreement is quite good over the whole wavelength range.

Figure 4 shows colour-colour diagrams of $(J - K)$ versus $(J - H)$, $(J - [3.6])$ and $(J - [4.5])$ (the latter two being representative for $(J - L)$ and $(J - M)$, respectively). The data are the mean *JHKLM* magnitudes of carbon and oxygen-rich stars based on the monitoring of the light curves from Le Bertre (1992, 1993) and Taranova & Shenavrin (2004). Only stars with magnitudes in all bands and without uncertain magnitudes were considered.

Although such a comparison between models and data is not trivial because of the effects of reddening (although most sources are within 2.5 kpc and reddening at these wavelengths

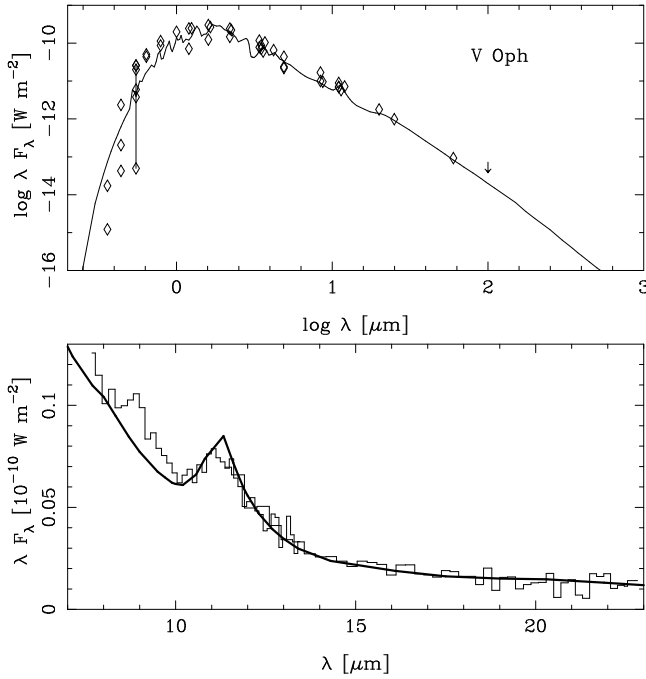
should be small) and the fact that the IRAC [3.6] and [4.5] filters are not directly comparable to *L* and *M*, it may nevertheless illustrate the overall correctness of the models, as suggested by the referee. Again, the overall agreement between models and data is quite good with most data points within 0.1 magnitude of any of the sequences.

The results of the models obtained in the present paper for the *V, I, J, H, K, IRAC, MIPS* and ASTRO-F magnitudes and fluxes are listed in Tables A.1 to A.26 for AGB stars and Tables A.27 to A.36 for post-AGB stars. Table A.1 is repeated as Table 2 to illustrate the content.

The AGB models have been calculated for mass loss rates up to a value resulting in a $(J - K)$ colour of about 10, roughly the reddest known AGB stars (Groenewegen et al. 1998). For every set of input in terms of stellar input spectrum and dust composition there are two tables, listing, respec-

Table 1. Adopted flux-densities for a zero-magnitude star

Filter	λ_0 (μm)	Flux (Jy)
IRAC_3.6	3.55	278.8
IRAC_4.5	4.49	179.6
IRAC_5.8	5.73	118.4
IRAC_8.0	7.87	63.5
MIPS_24	24	7.23
MIPS_70	70	0.791
MIPS_160	160	0.190
IRC_N2	2.69	651.4
IRC_N3	3.06	323.5
IRC_N4	4.55	199.8
MIRS_S7	8.0	84.5
MIRS_S9W	10.04	57.7
MIRS_S11	10.0	32.0
MIRL_L15	17.5	17.6
MIRL_L18W	17.6	11.0
MIRL_L24	23.55	7.45
FIS_N60	60	0.935
FIS_WIDE-S	90	0.604
FIS_WIDE-L	140	0.194
FIS_N160	160	0.166

**Fig. 3.** Model fit to the SED and IRAS LRS spectrum of the carbon Mira V Oph (cf. Groenewegen et al. 1998). Used is the 2650 K model atmosphere, $L = 4390 L_{\odot}$, $d = 0.68$ kpc, $\dot{M} = 3.0 \times 10^{-8} M_{\odot} \text{yr}^{-1}$, and a combination of 85% AMC and 15% SiC.

tively, V, I, J, H, K (in magnitudes) and the flux-densities (in mJy) for SPITZER IRAC and MIPS, and the flux-densities (in mJy) for the ASTRO-F IRC, MIR-S, MIR-L and FIS filters. Tables A.1-A.26 also list the mass loss rate and the dust optical depth, at $11.75 \mu\text{m}$ for AMC+SiC and $11.33 \mu\text{m}$ for AMC, $11.75 \mu\text{m}$ for AlOx and AlOx+silicate, and $10.20 \mu\text{m}$ for silicate. Optical depths at other wavelengths can be estimated from

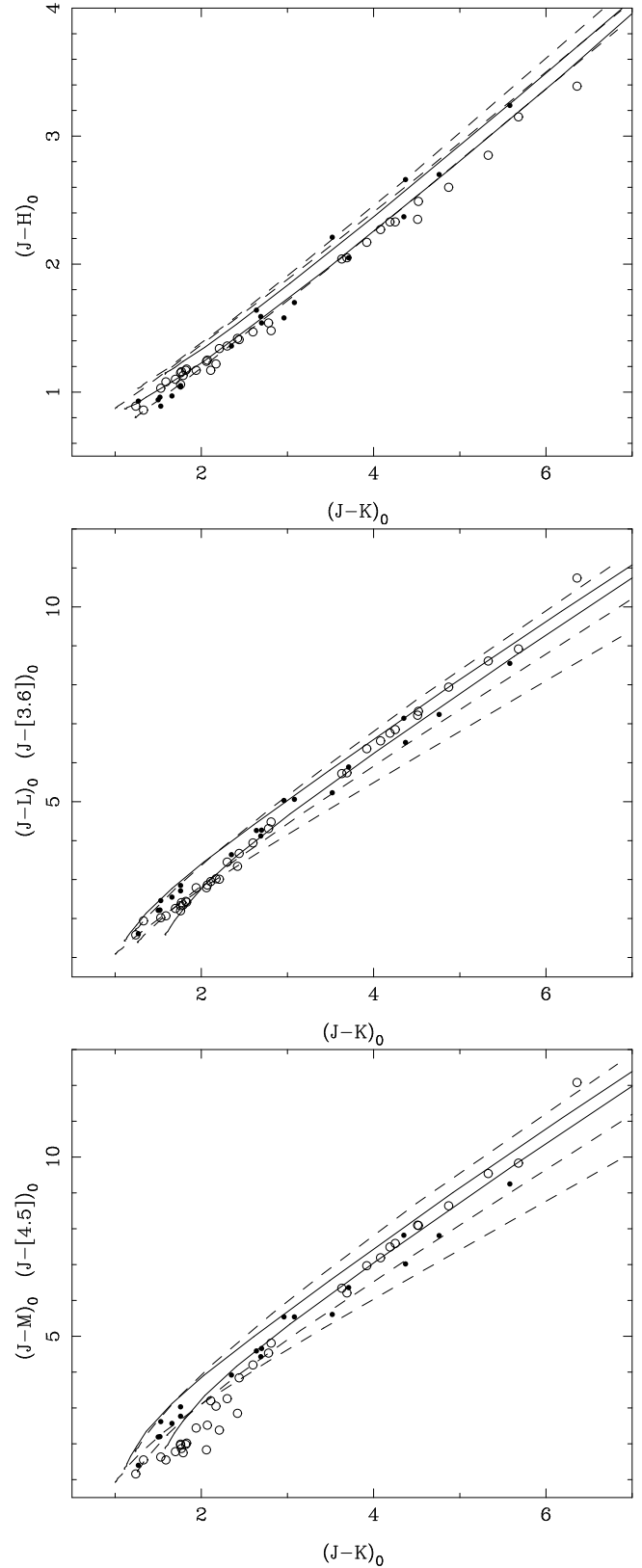
**Fig. 4.** Colour-Colour diagrams with $(J - K)$ plotted against $(J - H)$, $(J - [3.6])$ ($(J - L)$ for the observations), and $(J - [4.5])$ ($(J - M)$ for the observations). Carbon stars are plotted as open circles, oxygen-rich stars as filled circles. Shown are model sequences for carbon stars (solid lines) for $T_{\text{eff}} = 3600$ K, 85% AMC + 15% SiC dust, and $T_{\text{eff}} = 2650$ K, 100% AMC dust (the redder sequence), and oxygen-rich stars (dashed lines) for spectral type M0 and 100% AlOx dust, M6 and 40% silicate + 60% AlOx, and M10 and 100% silicate dust (from top to bottom for a given $(J - K)$).

Fig. 1. For the post-AGB models the dust temperature at the inner radius is listed instead of the mass loss rate. By decreasing this parameter the expansion of the dust envelope after cessation of mass loss at the end of the AGB can be simulated. The post-AGB tracks have only been calculated for the 100% silicate and 100% AMC models, as it appears that dust with appreciable amounts of, respectively, AlOx and SiC only appear at lower mass loss rates, and not at the tip of the AGB. The model runs are such that the first entry for the post-AGB models corresponds to the same parameter set as for the last entry in the corresponding AGB model (e.g. Tab. A.27-A.3, A.29-A.11, A.34-A.24) but listed as the result of an independent calculation. One can notice small differences of $\lesssim 1\%$ in the fluxes and this is due to the accuracy of the RT model at these large optical depths.

4.1. Scaling laws

The fluxes listed in the tables scale with $(L/3000)/(d/8.5)^2$ (and the magnitudes as $-2.5 \log$ of this factor).

The spectral energy distribution is—for a given stellar input spectrum—determined only by the dust optical depth, defined by (Groenewegen 1993, 1995):

$$\begin{aligned} \tau_\lambda &= \int_{r_{inner}}^{r_{outer}} \pi a^2 Q_\lambda n_d(r) dr = \\ &= 5.405 \cdot 10^8 \frac{\dot{M}}{R_\star} \frac{\Psi}{v_\infty} \frac{Q_\lambda/a}{\rho_d r_c} \int_1^{x_{max}} \frac{R(x)}{x^2} dx \end{aligned} \quad (2)$$

where n_d is the number density of dust particles, $x = r/r_c$ and $\dot{M}(r) = \dot{M} R(x)$. The units are: the (present-day) mass loss rate at the inner radius \dot{M} in $\text{M}_\odot \text{yr}^{-1}$, Ψ the dust-to-gas mass ratio, Q_λ/a the absorption coefficient of the dust over the grain radius in cm^{-1} , R_\star the stellar radius in solar radii, v_∞ the terminal velocity of the circumstellar envelope in km s^{-1} , ρ_d the dust grain density in gr cm^{-3} , r_c the inner dust radius in stellar radii and x_{max} the outer radius in units of r_c . For the assumptions adopted in the present paper—a constant velocity and mass loss rate, and a outer radius much larger than the inner radius—the integral becomes unity.

This relation implies a necessary scaling when the expansion velocity and/or dust-to-gas ratio and/or luminosity are different from the nominal ones, and this scaling is like $\dot{M} \sim (v/10 \text{ km s}^{-1}) (0.005/\Psi) \sqrt{L/3000}$.

4.2. Caveats

My expectation is that these tracks might be useful to identify AGB stars in colour-colour and colour-magnitude diagrams that will become available when SPITZER and ASTRO-F results on external galaxies become available. Such a comparison might also be useful to provide indications of the chemical type and dust optical depth. However, when doing such comparisons some limitations of the models must be kept in mind.

- AGB stars are variable, usually of the Semi-Regular or Mira type. Mira variables can have pulsation amplitudes corresponding to 6-8 magnitudes in V , and up to 2.5 mag

in K , 1.5 mag in M and 1.3 mag in N (e.g. Le Bertre 1992, 1993, Groenewegen et al. 1998). Little is known about the level of variability in the mid-IR, but for example CW Leo (IRC +10 216), with a full-amplitude in K of 2.0 mag (Le Bertre 1992), still has an full-amplitude at $850 \mu\text{m}$ of 0.24 mag (Jenness et al. 2002).

- Other dust components may be present that are not taken into account (MgS near $35 \mu\text{m}$ in carbon stars, e.g. Hony et al 2002, several crystalline silicate complexes near 23, 28, 33, 40 and $60 \mu\text{m}$, see e.g. Molster et al. 2002) and that may influence some fluxes, especially below $\sim 60 \mu\text{m}$.
 - The dust shell may be non-spherical and scattered light might play a role.
 - The models have been calculated assuming a constant mass loss rate. This may affect the far-IR colours (beyond $\sim 100 \mu\text{m}$) either way.
 - The photospheric models used are appropriate for solar metallicities. This implies possible shifts in colour for low optical depths where the photosphere dominate the colours in systems of non-solar metallicity.
 - The post-AGB model have been calculated under the assumption that the effective temperature and luminosity do not change over the time for the dust shell to drift away. For example, in the case of the 2650 K effective temperature C-rich central star, with a luminosity of $3000 L_\odot$ and 10 km s^{-1} expansion velocity it takes about 1100 year for the dust shell to expand to an inner dust radius temperature of 100 K, 8300 yr to 50 K, and 600 000 yr to 10 K.
- The transition timescale between the end of the AGB and the start of the PN phase (typically assumed to start at 10 000 K) is highly uncertain, and depends on the core mass (i.e. initial mass) of the star (the larger, the faster the evolution). Typical values are thought to be between 500 and 1500 years (e.g. Marigo et al. 2001, 2004).
- This implies that only for inner dust radius temperatures above $\gtrsim 150 \text{ K}$ the flow times scale is short enough for the assumption of constant luminosity and effective temperature likely to be valid.
- The final calibration may differ from the adopted one once the total throughput of the system has been established in-orbit.

5. Discussion

Dust radiative transfer models for (post-)AGB stars are presented from the optical to the far-infrared. The models are calculated in view of the (upcoming) results from SPITZER and (hopefully) ASTRO-F. They may be useful to identify AGB stars, and provide rough estimates of spectral type, luminosity and mass loss rate. I warn again, though, that once candidate AGB stars have been selected, the *best* estimates for mass loss rate, luminosity and dust composition can only be obtained by detailed fitting of the entire SED (and spectra if available) of individual stars.

As an illustration, Figs. 5 and 6 show some tracks in a colour-magnitude diagram for, respectively, SPITZER IRAC filters for an AGB star of $3000 L_\odot$ at a distance of 932 Kpc (appropriate for WLM, McConnachie et al. 2005), and SPITZER

Table 2. Optical, NIR, IRAC and MIPS magnitudes and fluxes for a C-rich AGB star, $T_{\text{eff}} = 2650$ K, 85% AMC + 15% SiC. All tables are available on-line in Appendix A as Table A.1-A.36. In all tables \dot{M} represents the mass loss rate in $M_{\odot}\text{yr}^{-1}$, while τ represents the dust optical depth at the wavelengths listed in Sect. 4.

\dot{M}	τ	V	I	J	H	K	3.6	4.5	5.8	8.0	24	70	160
0.10E-09	0.000045	13.85	10.99	9.07	7.92	7.49	282.3	236.6	140.1	69.2	23.36	2.91	0.773
0.25E-09	0.000113	13.85	10.99	9.07	7.92	7.49	282.5	236.9	140.3	69.4	23.42	2.92	0.776
0.50E-09	0.000226	13.85	10.99	9.07	7.92	7.49	282.9	237.3	140.7	69.7	23.51	2.93	0.781
0.10E-08	0.000452	13.85	11.00	9.07	7.92	7.49	283.6	238.1	141.5	70.5	23.71	2.97	0.790
0.25E-08	0.001130	13.86	11.00	9.07	7.93	7.49	285.9	240.5	143.8	72.6	24.28	3.08	0.817
0.50E-08	0.002259	13.87	11.01	9.08	7.93	7.49	289.7	244.6	147.7	76.1	25.24	3.26	0.863
0.10E-07	0.004513	13.89	11.02	9.08	7.93	7.49	297.2	252.7	155.4	83.1	27.14	3.62	0.953
0.25E-07	0.011247	13.96	11.07	9.11	7.95	7.48	319.2	276.5	178.3	103.7	32.77	4.69	1.223
0.50E-07	0.022382	14.08	11.15	9.16	7.98	7.48	354.4	314.8	215.1	137.2	41.92	6.43	1.663
0.10E-06	0.044342	14.31	11.31	9.25	8.03	7.49	418.4	385.8	284.2	200.4	59.44	9.75	2.498
0.25E-06	0.108009	14.98	11.76	9.53	8.19	7.52	574.2	566.0	464.3	367.7	106.66	18.76	4.778
0.50E-06	0.208266	16.02	12.47	9.96	8.46	7.61	747.2	786.7	698.1	592.6	173.15	31.57	8.023
0.10E-05	0.393236	17.91	13.78	10.77	8.99	7.85	913.5	1054.0	1018.6	923.7	281.23	52.72	13.390
0.20E-05	0.725089	21.26	16.12	12.23	9.97	8.40	955.8	1270.3	1375.0	1355.7	455.47	87.87	22.354
0.40E-05	1.306390	26.92	20.19	14.77	11.71	9.47	775.9	1287.4	1647.3	1839.5	746.08	149.40	38.197
0.60E-05	1.825759	31.81	23.78	16.99	13.21	10.42	587.2	1164.4	1699.8	2097.6	1002.97	206.71	53.101
0.10E-04	2.756648	40.25	30.11	20.72	15.67	12.01	341.1	893.9	1602.9	2320.3	1458.59	315.02	81.643

MIPS filters for an AGB star of $3000 L_{\odot}$ at a distance of 785 Kpc (appropriate for M31, McConnachie et al. 2005). WLM and M31 are actual targets for those instruments according to the Spitzer Reserved Observations Catalog. One can observe that the tracks of the C- and O-rich mass-loss sequence largely overlap in [3.6-4.5] colour. Also the post-AGB tracks cover the same range in this colour. On the other hand, the [3.6] magnitude is a good indicator of the luminosity and the [3.6-4.5] colours of the mass loss rate. By comparison, in Figure 6 C- and O-rich models separate, as well as AGB from post-AGB models. This illustrates the usefulness of a $70 \mu\text{m}$ filter to trace post-AGB evolution. The MIPS $24 \mu\text{m}$ filter traces the wing of the silicate $18 \mu\text{m}$ feature and therefore the $24 \mu\text{m}$ magnitude brightens quickly with the onset of mass-loss, so that the [24-70] colour initially becomes negative for O-rich stars. On the other hand, luminosity and mass loss rate are difficult to discriminate as the AGB sequence is almost vertical in [24-70] colour.

Acknowledgements. I would like to thanks Issei Yamamura (Institute of Space and Astronomical Science, ISAS, Kanagawa, Japan) for pointing out the availability of the ASTRO-F filter curves, and Leen Decin (K.U. Leuven) for providing a MARCS code model atmosphere for Vega. Joris Blommaert is thanked for reading an earlier version of the paper.

References

- Begemann, B., Dorschner, J., & Henning, Th., et al. 1997, ApJ 476, 199
- Beichman, C.A., Neugebauer, G., Habing, H.J., et al. 1988, IRAS Explanatory Supplement, NASA RP-1190
- Blommaert, J.A.D.L., Omont, A., The ISO GAL collaboration 2000, Mem. Soc. Astron. Ital. 71, 623
- Blommaert, J.A.D.L., 2003, in: "Exploiting the ISO Data Archive. Infrared Astronomy in the Internet Age", Eds. C. Gry, S. Peschke, J. Matagne, P. Garcia-Lario, R. Lorente, & A. Salama, ESA SP-511, p. 81.
- Blommaert, J.A.D.L., Siebenmoregen, R., Coulais, A., et al. 2003, The ISO handbook, volume II, ESA-SP 1262
- Cesarsky, C.J., Abergel, A., Agnese, P., et al. 1996, A&A 315, L32
- David, P., & Pégourié, B. 1995, A&A 293, 833
- Fazio, G., Hora, J.L., & Allen, L.E. 2004, ApJS 154, 1
- Fluks, M.A., Plez, B., Thé, P.S., et al. 1994, A&AS 105, 311

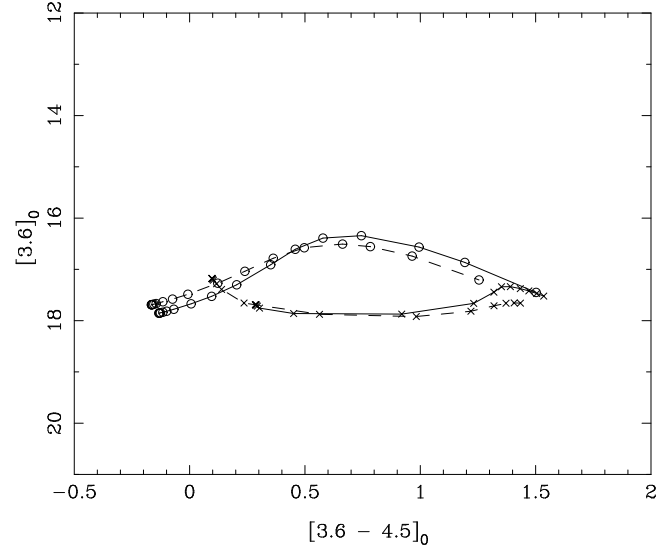


Fig. 5. IRAC colour-magnitude diagram for models with $3000 L_{\odot}$ at 932 Kpc. The following sequences of increasing mass loss are shown: Carbon-rich AGB star with $T_{\text{eff}} = 3600$ K, and 85% AMC + 15% SiC (circles & solid line), Carbon-rich post-AGB star with $T_{\text{eff}} = 2650$ K, and 100% AMC (crosses & solid line), Oxygen-rich AGB star with $T_{\text{eff}} = 3297$ K, and 60% silicate + 40% AlOx (circles & dashed line), and Oxygen-rich post-AGB star with $T_{\text{eff}} = 2500$ K, and 100% silicate (crosses & dashed line).

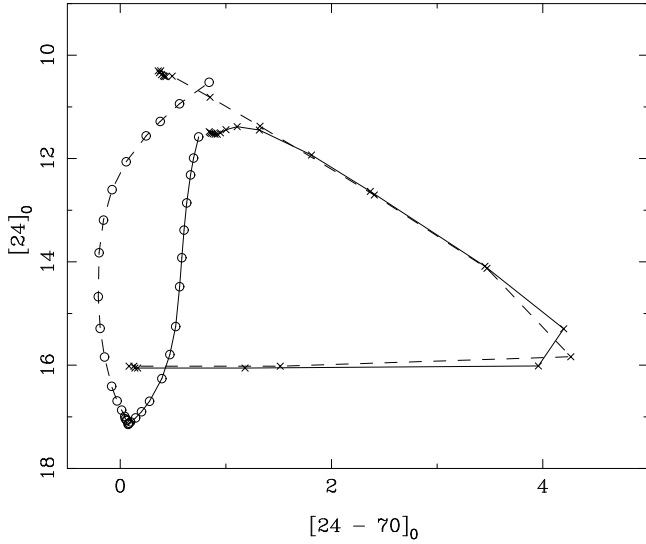


Fig. 6. MIPS colour-magnitude diagram for models with 3000 L_{\odot} at 785 Kpc. Model tracks as in Fig. 5.

Groenewegen, M.A.T. 1993, Ph.D. Thesis, Chapter 5, University of Amsterdam (available at <http://www.ster.kuleuven.ac.be/~groen/thesis.ps.gz>)

Groenewegen, M.A.T. 1994a, A&A 282, 115

Groenewegen, M.A.T. 1994b, A&A 290, 544

Groenewegen, M.A.T. 1995, A&A 293, 463

Groenewegen, M.A.T. 1997, A&A 317, 503

Groenewegen, M.A.T., & Blommaert, J.A.D.L. 1998, A&A 332, 25

Groenewegen, M.A.T., Oudmaijer, R.D., & Ludwig, H.-G. 1997, MNRAS 292, 686

Groenewegen, M.A.T., Smith, C.H., Wood, P.R., Omont, A., & Fujiyoshi, T. 1995, ApJ 449, L119

Groenewegen, M.A.T., Whitelock, P.A., Smith, C.H., & Kerschbaum, F. 1998, MNRAS 293, 18

Hony, S., Waters, L.B.F.M., & Tielens, A.G.G.M. 2002, A&A 390, 533

Ivezic, Z., Groenewegen, M.A.T., Me'shchikov, A., Szczerba, R. 1997, MNRAS 291, 121

Jennens, T., Stevens, J.A., Archibald, E.N., et al. 2002, MNRAS 336, 14

Le Bertre, T. 1992, A&AS 94, 377

Le Bertre, T. 1993, A&AS 97, 729

Loidl, R., Lançon, A., & Jørgensen, U.G. 2001, A&A 371, 1065

Loup, C., Cioni, M.-R., Blommaert, J.A.D.L., et al. 1999a, in: "The Universe as seen by ISO", Eds. P. Cox & M.F. Kessler, ESA SP-427, p. 369

Loup, C., Josselin, E., Cioni, M.-R., et al. 1999b, IAU Symposium 191, Eds. T. Le Bertre, A. Lebre, and C. Waelkens, p. 561

Loup, C., Zijlstra, A.A., Waters, L.B.F.M., & Groenewegen, M.A.T. 1997, A&AS 125, 419

Marigo, P., Girardi, L., Groenewegen, M.A.T., & Weiss, A. 2001, A&A 378, 958

Marigo, P., Girardi, L., Weiss, A., Groenewegen, M.A.T., & Chiosi, C., 2004, A&A 423, 995

Matsuhara, H., Shibai, H., Onaka, T., Usui, F., Advances in Space Research, accepted, (astro-ph/0507157)

McConnachie, A.W., Irwin, M.J., Ferguson, A.M.N., et al. 2005, MNRAS 356, 979

Molster, F.J., Waters, L.B.F.M., & Tielens, A.G.G.M. 2002, A&A 382, 222

Ojha, D.K., Omont, A., Schuller, F., Simon, G., Ganesh, S., & Schultheis, M. 2003, A&A 403, 151

Omont, A., Ganesh, S., Alard, C., et al. 1999, A&A 348, 755

Omont, A., Gilmore, G.F., Alard, C., et al. 2003, A&A 403, 975

Ortiz, R., Blommaert, J.A.D.L., Copet, E., et al. 2002, A&A 388, 792

Pearson, C.P., Matsumoto, H.S., Murukami, H., et al. 2004, MNRAS 347, 1113

Pégourié, B. 1988, A&A 194, 335

Reid, N. 1991, ApJ 382, 143

Reid, N., Tinney, C., & Mould, J. 1990, ApJ 348, 98

Rieke, G., Young, E.T., & Engelbracht, C.W. 2004, ApJS 154, 1

Rouleau, F., & Martin, P.G. 1991, ApJ 377, 526

Taranova, O.G., Shenavrin V.I. 2004, PAZh 30, 605

Trams, N.R., Van Loon, J.Th., Waters, L.B.F.M., et al. 1999, A&A 346, 843

van der Veen, W.E.C.J., & Habing, H.J. 1988, A&A 194, 125

van Loon, J.Th., Groenewegen, M.A.T., de Koter, A., et al. 1999, A&A 351, 559

Werner, M., Roellig, T., Low, F., et al. 2004, ApJS 154, 1

Whitelock, P.A., Feast, M.W., Menzies, J.W., & Catchpole, R.M. 1989, MNRAS 238, 769

Wood, P.R., Whiteoak, J.B., Hughes, S.M.G., et al. 1992, ApJ 397, 552

Zijlstra, A.A., Loup, C., Waters, L.B.F.M., et al. 1996, MNRAS 279, 32

Appendix A: Tabular material

Table A.1. Optical, NIR, IRAC and MIPS magnitudes and fluxes for a C-rich AGB star, $T_{\text{eff}} = 2650$ K, 85% AMC + 15% SiC.

\dot{M}	τ	V	I	J	H	K	3.6	4.5	5.8	8.0	24	70	160
0.10E-09	0.000045	13.85	10.99	9.07	7.92	7.49	282.3	236.6	140.1	69.2	23.36	2.91	0.773
0.25E-09	0.000113	13.85	10.99	9.07	7.92	7.49	282.5	236.9	140.3	69.4	23.42	2.92	0.776
0.50E-09	0.000226	13.85	10.99	9.07	7.92	7.49	282.9	237.3	140.7	69.7	23.51	2.93	0.781
0.10E-08	0.000452	13.85	11.00	9.07	7.92	7.49	283.6	238.1	141.5	70.5	23.71	2.97	0.790
0.25E-08	0.001130	13.86	11.00	9.07	7.93	7.49	285.9	240.5	143.8	72.6	24.28	3.08	0.817
0.50E-08	0.002259	13.87	11.01	9.08	7.93	7.49	289.7	244.6	147.7	76.1	25.24	3.26	0.863
0.10E-07	0.004513	13.89	11.02	9.08	7.93	7.49	297.2	252.7	155.4	83.1	27.14	3.62	0.953
0.25E-07	0.011247	13.96	11.07	9.11	7.95	7.48	319.2	276.5	178.3	103.7	32.77	4.69	1.223
0.50E-07	0.022382	14.08	11.15	9.16	7.98	7.48	354.4	314.8	215.1	137.2	41.92	6.43	1.663
0.10E-06	0.044342	14.31	11.31	9.25	8.03	7.49	418.4	385.8	284.2	200.4	59.44	9.75	2.498
0.25E-06	0.108009	14.98	11.76	9.53	8.19	7.52	574.2	566.0	464.3	367.7	106.66	18.76	4.778
0.50E-06	0.208266	16.02	12.47	9.96	8.46	7.61	747.2	786.7	698.1	592.6	173.15	31.57	8.023
0.10E-05	0.393236	17.91	13.78	10.77	8.99	7.85	913.5	1054.0	1018.6	923.7	281.23	52.72	13.390
0.20E-05	0.725089	21.26	16.12	12.23	9.97	8.40	955.8	1270.3	1375.0	1355.7	455.47	87.87	22.354
0.40E-05	1.306390	26.92	20.19	14.77	11.71	9.47	775.9	1287.4	1647.3	1839.5	746.08	149.40	38.197
0.60E-05	1.825759	31.81	23.78	16.99	13.21	10.42	587.2	1164.4	1699.8	2097.6	1002.97	206.71	53.101
0.10E-04	2.756648	40.25	30.11	20.72	15.67	12.01	341.1	893.9	1602.9	2320.3	1458.59	315.02	81.643

Table A.2. Optical, NIR, IRAC and MIPS magnitudes and fluxes for a C-rich AGB star, $T_{\text{eff}} = 3600$ K, 85% AMC + 15% SiC.

\dot{M}	τ	V	I	J	H	K	3.6	4.5	5.8	8.0	24	70	160
0.10E-09	0.000040	12.01	10.41	9.08	8.21	7.97	241.7	137.7	94.5	61.8	8.53	1.00	0.264
0.25E-09	0.000099	12.01	10.41	9.08	8.21	7.97	241.9	138.0	94.8	62.0	8.60	1.01	0.267
0.50E-09	0.000198	12.01	10.41	9.08	8.21	7.97	242.4	138.5	95.3	62.4	8.71	1.03	0.272
0.10E-08	0.000395	12.01	10.41	9.08	8.21	7.97	243.3	139.5	96.2	63.3	8.93	1.07	0.283
0.25E-08	0.000988	12.02	10.41	9.08	8.21	7.97	246.0	142.4	98.9	65.7	9.59	1.20	0.315
0.50E-08	0.001975	12.03	10.42	9.09	8.22	7.96	250.6	147.3	103.5	69.8	10.70	1.41	0.367
0.10E-07	0.003946	12.05	10.44	9.10	8.22	7.96	259.6	157.0	112.5	77.8	12.88	1.82	0.471
0.25E-07	0.009838	12.11	10.48	9.12	8.23	7.94	285.8	185.2	139.0	101.5	19.32	3.04	0.778
0.50E-07	0.019587	12.22	10.55	9.16	8.25	7.91	327.3	230.2	181.3	139.4	29.63	5.00	1.275
0.10E-06	0.038832	12.42	10.69	9.24	8.28	7.88	402.7	313.1	259.7	210.0	48.90	8.68	2.217
0.25E-06	0.094927	13.02	11.09	9.48	8.40	7.82	577.3	514.1	455.4	389.4	99.39	18.26	4.628
0.50E-06	0.184005	13.96	11.72	9.86	8.62	7.83	762.8	749.3	696.8	618.1	166.73	31.23	7.911
0.10E-05	0.350641	15.71	12.91	10.60	9.07	7.99	932.6	1023.2	1013.8	941.3	272.66	52.03	13.202
0.20E-05	0.655079	18.85	15.07	11.95	9.97	8.46	973.2	1244.4	1360.9	1357.9	443.01	86.54	22.008
0.40E-05	1.199514	24.31	18.91	14.38	11.62	9.46	792.4	1275.7	1633.9	1833.1	730.54	147.59	37.749
0.60E-05	1.693328	29.09	22.36	16.55	13.08	10.37	602.1	1163.6	1693.5	2092.2	985.61	204.49	52.562
0.10E-04	2.589452	37.43	28.55	20.29	15.53	11.94	351.2	902.2	1607.5	2321.2	1438.34	311.89	80.904

Table A.3. Optical, NIR, IRAC and MIPS magnitudes and fluxes for a C-rich AGB star, $T_{\text{eff}} = 2650$ K, 100% AMC.

\dot{M}	τ	V	I	J	H	K	3.6	4.5	5.8	8.0	24	70	160
0.10E-09	0.000017	13.85	10.99	9.07	7.92	7.49	282.3	236.6	140.1	69.2	23.37	2.91	0.775
0.25E-09	0.000043	13.85	10.99	9.07	7.92	7.49	282.5	236.9	140.4	69.5	23.43	2.92	0.779
0.50E-09	0.000086	13.85	10.99	9.07	7.92	7.49	282.9	237.4	140.8	69.9	23.54	2.94	0.787
0.10E-08	0.000172	13.85	11.00	9.07	7.92	7.49	283.7	238.2	141.7	70.7	23.75	2.99	0.802
0.25E-08	0.000429	13.86	11.00	9.07	7.93	7.49	286.2	240.9	144.4	73.2	24.40	3.13	0.848
0.50E-08	0.000857	13.87	11.01	9.08	7.93	7.49	290.2	245.4	148.8	77.3	25.48	3.35	0.923
0.10E-07	0.001712	13.90	11.03	9.09	7.93	7.48	298.2	254.2	157.6	85.5	27.61	3.80	1.075
0.25E-07	0.004267	13.98	11.08	9.12	7.95	7.48	321.7	280.3	183.5	109.7	33.93	5.13	1.523
0.50E-07	0.008490	14.11	11.17	9.17	7.98	7.48	359.1	322.1	225.1	148.7	44.17	7.29	2.251
0.10E-06	0.016815	14.36	11.34	9.27	8.03	7.48	426.6	399.0	302.9	222.2	63.69	11.42	3.650
0.25E-06	0.040938	15.09	11.83	9.55	8.20	7.51	588.9	591.8	502.8	414.3	115.82	22.49	7.454
0.50E-06	0.078906	16.23	12.60	10.01	8.48	7.60	764.9	822.7	757.1	667.8	188.45	38.07	12.895
0.10E-05	0.148964	18.31	14.02	10.88	9.03	7.85	927.6	1094.1	1096.6	1033.6	305.85	63.65	21.981
0.20E-05	0.274773	21.97	16.57	12.43	10.05	8.41	958.4	1301.5	1460.3	1500.1	495.57	106.17	37.261
0.40E-05	0.495402	28.14	20.98	15.13	11.85	9.50	766.9	1296.6	1715.4	2002.4	811.57	180.12	64.030
0.60E-05	0.692600	33.45	24.88	17.47	13.40	10.46	575.6	1158.3	1742.5	2251.6	1087.46	247.77	88.634
0.10E-04	1.046017	42.60	31.69	21.34	15.90	12.05	330.5	872.2	1600.6	2429.9	1566.50	372.35	134.189

Table A.4. Optical, NIR, IRAC and MIPS magnitudes and fluxes for a C-rich AGB star, $T_{\text{eff}} = 3600$ K, 100% AMC.

\dot{M}	τ	V	I	J	H	K	3.6	4.5	5.8	8.0	24	70	160
0.10E-09	0.000015	12.01	10.41	9.08	8.21	7.97	241.7	137.8	94.6	61.8	8.54	1.00	0.266
0.25E-09	0.000037	12.01	10.41	9.08	8.21	7.97	242.0	138.1	94.9	62.1	8.61	1.02	0.271
0.50E-09	0.000074	12.01	10.41	9.08	8.21	7.97	242.5	138.6	95.4	62.6	8.74	1.04	0.280
0.10E-08	0.000149	12.01	10.41	9.08	8.21	7.97	243.4	139.7	96.5	63.6	8.99	1.10	0.297
0.25E-08	0.000372	12.02	10.41	9.08	8.21	7.97	246.4	142.9	99.6	66.4	9.74	1.25	0.350
0.50E-08	0.000743	12.03	10.42	9.09	8.22	7.96	251.3	148.3	104.8	71.3	10.99	1.52	0.438
0.10E-07	0.001485	12.05	10.44	9.10	8.22	7.96	260.9	159.0	115.1	80.8	13.46	2.04	0.613
0.25E-07	0.003703	12.12	10.48	9.12	8.23	7.94	289.1	190.1	145.3	108.7	20.72	3.56	1.128
0.50E-07	0.007372	12.24	10.56	9.16	8.25	7.91	333.3	239.3	193.4	153.1	32.32	6.00	1.954
0.10E-06	0.014614	12.46	10.71	9.25	8.28	7.87	413.2	329.3	281.7	235.2	53.84	10.55	3.504
0.25E-06	0.035722	13.11	11.14	9.50	8.40	7.81	595.1	544.3	499.1	441.4	109.59	22.37	7.588
0.50E-06	0.069241	14.14	11.83	9.91	8.63	7.82	783.3	789.6	760.7	698.2	182.82	38.08	13.122
0.10E-05	0.132019	16.04	13.11	10.68	9.10	7.99	948.1	1066.2	1094.8	1053.8	297.51	63.16	22.088
0.20E-05	0.246947	19.47	15.45	12.12	10.04	8.47	976.5	1277.9	1448.1	1503.1	482.93	104.93	37.149
0.40E-05	0.452970	25.42	19.61	14.69	11.74	9.48	784.0	1287.6	1705.0	1997.9	795.70	178.35	63.767
0.60E-05	0.640216	30.61	23.35	16.99	13.25	10.41	590.6	1159.8	1739.9	2249.6	1069.91	245.60	88.248
0.10E-04	0.979777	39.63	30.04	20.91	15.75	11.98	340.6	882.0	1608.9	2435.3	1546.00	369.13	133.436

Table A.5. Optical, NIR, IRAC and MIPS magnitudes and fluxes for a O-rich AGB star, $T_{\text{eff}} = 3850$ K, 100% AlOx.

\dot{M}	τ	V	I	J	H	K	3.6	4.5	5.8	8.0	24	70	160
0.10E-09	0.000200	11.84	10.19	9.08	8.21	8.08	177.3	98.3	69.8	42.2	5.35	0.61	0.150
0.25E-09	0.000499	11.84	10.19	9.08	8.21	8.08	177.4	98.3	69.8	42.3	5.45	0.62	0.153
0.50E-09	0.000998	11.84	10.19	9.08	8.21	8.08	177.4	98.4	69.8	42.4	5.61	0.64	0.158
0.10E-08	0.001996	11.84	10.19	9.08	8.21	8.08	177.5	98.5	70.0	42.6	5.93	0.68	0.167
0.25E-08	0.004989	11.84	10.19	9.09	8.21	8.08	177.7	98.7	70.3	43.4	6.90	0.78	0.196
0.50E-08	0.009974	11.85	10.19	9.09	8.21	8.08	178.1	99.1	70.8	44.7	8.52	0.95	0.244
0.10E-07	0.019932	11.85	10.20	9.09	8.21	8.08	178.8	100.0	71.9	47.3	11.74	1.30	0.339
0.25E-07	0.049715	11.88	10.21	9.09	8.21	8.07	181.1	102.5	75.3	55.0	21.39	2.33	0.627
0.50E-07	0.099054	11.91	10.23	9.10	8.21	8.07	184.9	106.7	80.8	67.8	37.33	4.06	1.106
0.10E-06	0.196662	11.99	10.28	9.13	8.22	8.05	192.6	115.1	92.0	93.1	68.75	7.51	2.068
0.25E-06	0.482194	12.20	10.41	9.18	8.23	8.02	214.9	139.8	124.3	164.5	156.71	17.68	4.914
0.50E-06	0.938610	12.53	10.62	9.28	8.26	7.97	250.9	179.6	176.4	273.6	288.94	34.25	9.596
0.10E-05	1.801754	13.17	11.02	9.46	8.31	7.89	316.7	253.2	271.5	455.0	506.90	65.84	18.649
0.20E-05	3.412976	14.35	11.77	9.83	8.45	7.81	425.5	378.0	430.5	710.0	820.13	123.70	35.612
0.40E-05	6.387136	16.50	13.14	10.55	8.79	7.78	577.7	563.4	661.3	980.2	1210.06	226.76	66.781
0.60E-05	9.165066	18.49	14.42	11.26	9.16	7.84	675.9	694.7	820.4	1102.5	1472.19	321.68	96.278
0.10E-04	14.355180	22.12	16.79	12.59	9.89	8.04	785.0	866.6	1022.8	1191.9	1863.47	501.90	153.686
0.20E-04	26.049158	30.00	22.04	15.52	11.54	8.65	854.2	1061.5	1247.4	1218.2	2556.48	926.85	293.597

Table A.6. Optical, NIR, IRAC and MIPS magnitudes and fluxes for a O-rich AGB star, $T_{\text{eff}} = 3297$ K, 100% AlOx.

\dot{M}	τ	V	I	J	H	K	3.6	4.5	5.8	8.0	24	70	160
0.10E-09	0.000242	14.31	11.11	8.88	7.85	7.62	281.1	155.5	112.1	68.8	9.11	1.05	0.258
0.25E-09	0.000604	14.31	11.11	8.88	7.85	7.62	281.1	155.5	112.1	68.9	9.19	1.06	0.261
0.50E-09	0.001209	14.31	11.11	8.88	7.85	7.62	281.2	155.5	112.1	69.0	9.32	1.08	0.265
0.10E-08	0.002417	14.31	11.11	8.88	7.85	7.62	281.2	155.6	112.2	69.2	9.58	1.10	0.272
0.25E-08	0.006041	14.31	11.11	8.88	7.85	7.62	281.4	155.8	112.5	69.8	10.37	1.19	0.296
0.50E-08	0.012076	14.32	11.11	8.88	7.85	7.62	281.6	156.1	112.9	70.8	11.68	1.33	0.335
0.10E-07	0.024129	14.33	11.12	8.88	7.85	7.62	282.2	156.7	113.8	72.9	14.30	1.61	0.413
0.25E-07	0.060160	14.35	11.13	8.89	7.86	7.62	283.8	158.7	116.4	79.0	22.17	2.47	0.650
0.50E-07	0.119790	14.40	11.16	8.91	7.86	7.62	286.5	161.9	120.8	89.3	35.25	3.90	1.047
0.10E-06	0.237577	14.49	11.21	8.93	7.88	7.62	292.1	168.5	129.6	109.4	60.86	6.77	1.843
0.25E-06	0.580645	14.75	11.37	9.02	7.92	7.61	309.1	188.6	156.4	168.9	135.54	15.55	4.286
0.50E-06	1.125672	15.16	11.61	9.14	7.98	7.61	337.9	222.4	201.1	262.1	250.59	30.35	8.428
0.10E-05	2.149076	15.92	12.07	9.39	8.09	7.59	393.5	288.0	286.7	423.2	448.07	59.71	16.742
0.20E-05	4.038786	17.33	12.92	9.84	8.31	7.59	490.8	405.5	437.3	660.2	747.86	115.83	32.964
0.40E-05	7.465082	19.84	14.45	10.69	8.75	7.64	632.6	587.6	664.3	923.8	1144.26	218.76	63.673
0.60E-05	10.610692	22.10	15.86	11.48	9.18	7.74	725.0	718.5	822.6	1048.4	1417.68	314.37	93.074
0.10E-04	16.384277	26.11	18.40	12.94	9.99	8.00	824.9	888.9	1023.3	1147.3	1826.46	496.12	150.500
0.20E-04	29.073149	34.21	23.76	15.94	11.70	8.67	875.4	1075.5	1243.0	1195.3	2543.47	923.50	290.248

Table A.7. Optical, NIR, IRAC and MIPS magnitudes and fluxes for a O-rich AGB star, $T_{\text{eff}} = 2500$ K, 100% AlOx.

\dot{M}	τ	V	I	J	H	K	3.6	4.5	5.8	8.0	24	70	160
0.10E-09	0.000258	17.04	12.72	8.67	7.87	7.44	451.6	318.0	247.5	152.9	24.16	2.86	0.703
0.25E-09	0.000644	17.04	12.72	8.67	7.87	7.44	451.6	318.1	247.5	153.0	24.23	2.86	0.705
0.50E-09	0.001287	17.04	12.72	8.67	7.87	7.44	451.6	318.1	247.5	153.0	24.34	2.88	0.709
0.10E-08	0.002575	17.04	12.72	8.67	7.87	7.44	451.7	318.1	247.6	153.2	24.57	2.90	0.716
0.25E-08	0.006435	17.04	12.72	8.67	7.87	7.44	451.8	318.3	247.8	153.7	25.25	2.98	0.737
0.50E-08	0.012865	17.05	12.72	8.68	7.87	7.44	452.0	318.5	248.1	154.5	26.40	3.10	0.773
0.10E-07	0.025708	17.06	12.73	8.68	7.87	7.44	452.3	319.0	248.8	156.2	28.68	3.36	0.844
0.25E-07	0.064110	17.09	12.75	8.69	7.88	7.44	453.4	320.4	250.8	161.2	35.55	4.13	1.059
0.50E-07	0.127692	17.13	12.77	8.71	7.89	7.44	455.3	322.8	254.2	169.5	47.00	5.43	1.422
0.10E-06	0.253438	17.23	12.82	8.74	7.90	7.44	459.2	327.8	261.2	186.1	69.54	8.03	2.151
0.25E-06	0.620454	17.50	12.97	8.83	7.95	7.45	471.5	343.5	282.8	235.9	135.98	16.11	4.411
0.50E-06	1.205401	17.92	13.21	8.98	8.02	7.46	493.1	370.6	319.7	315.1	239.85	29.90	8.287
0.10E-05	2.307303	18.72	13.66	9.26	8.15	7.47	536.6	425.0	392.6	455.1	421.76	57.75	16.188
0.20E-05	4.345098	20.18	14.50	9.77	8.39	7.50	615.0	525.1	523.9	664.6	705.30	112.05	31.883
0.40E-05	8.036496	22.75	16.04	10.71	8.87	7.60	730.5	683.4	726.0	902.2	1094.96	214.00	62.263
0.60E-05	11.411263	25.00	17.44	11.57	9.32	7.73	804.4	798.0	868.6	1018.6	1374.44	310.41	91.843
0.10E-04	17.578022	28.84	19.96	13.13	10.17	8.02	879.4	946.7	1050.9	1118.5	1802.26	496.19	150.366
0.20E-04	31.022861	35.94	24.96	16.23	11.90	8.72	899.3	1106.3	1253.9	1180.5	2551.99	936.16	293.890

Table A.8. Optical, NIR, IRAC and MIPS magnitudes and fluxes for a O-rich AGB star, $T_{\text{eff}} = 3850$ K, 60% Silicate + 40% Alox.

\bar{M}	τ	V	I	J	H	K	3.6	4.5	5.8	8.0	24	70	160
0.10E-09	0.000145	11.84	10.19	9.08	8.21	8.08	177.4	98.4	69.8	42.2	5.38	0.61	0.150
0.25E-09	0.000362	11.84	10.19	9.08	8.21	8.08	177.5	98.5	69.9	42.4	5.53	0.63	0.154
0.50E-09	0.000725	11.84	10.19	9.08	8.21	8.08	177.8	98.7	70.1	42.7	5.77	0.65	0.160
0.10E-08	0.001449	11.84	10.19	9.09	8.21	8.08	178.2	99.2	70.5	43.3	6.26	0.69	0.172
0.25E-08	0.003621	11.85	10.19	9.09	8.21	8.08	179.5	100.4	71.7	45.0	7.71	0.81	0.207
0.50E-08	0.007239	11.86	10.20	9.09	8.21	8.07	181.6	102.5	73.7	47.9	10.11	1.02	0.266
0.10E-07	0.014465	11.88	10.21	9.09	8.21	8.07	185.9	106.8	77.7	53.7	14.89	1.42	0.384
0.25E-07	0.036064	11.94	10.24	9.11	8.21	8.05	198.4	119.2	89.3	70.7	28.98	2.62	0.731
0.50E-07	0.071808	12.04	10.30	9.13	8.21	8.02	218.5	139.1	108.2	97.9	51.63	4.56	1.294
0.10E-06	0.142381	12.23	10.41	9.17	8.22	7.98	256.0	176.8	143.8	148.6	94.19	8.23	2.368
0.25E-06	0.348180	12.80	10.73	9.31	8.26	7.89	347.7	270.5	233.6	272.6	204.27	18.30	5.355
0.50E-06	0.675066	13.69	11.24	9.54	8.35	7.82	461.8	393.0	354.0	429.3	353.31	32.95	9.781
0.10E-05	1.287621	15.33	12.19	10.00	8.58	7.81	608.3	566.4	533.5	643.9	586.79	59.13	17.825
0.20E-05	2.408700	18.27	13.92	10.88	9.07	7.96	752.3	777.8	776.6	906.0	941.60	107.60	32.929
0.40E-05	4.416763	23.29	16.98	12.48	10.03	8.39	819.6	975.4	1059.8	1189.9	1475.34	201.12	62.428
0.60E-05	6.234009	27.61	19.68	13.90	10.89	8.85	790.8	1046.7	1215.5	1348.4	1902.40	293.31	91.798
0.10E-04	9.513249	34.98	24.39	16.28	12.34	9.66	676.1	1053.7	1358.4	1515.0	2593.56	474.96	150.303
0.20E-04	16.500765	46.83	32.09	20.19	14.81	11.16	442.9	903.3	1391.4	1630.5	3810.67	907.69	292.349

Table A.9. Optical, NIR, IRAC and MIPS magnitudes and fluxes for a O-rich AGB star, $T_{\text{eff}} = 3297$ K, 60% Silicate + 40% Alox.

\bar{M}	τ	V	I	J	H	K	3.6	4.5	5.8	8.0	24	70	160
0.10E-09	0.000177	14.31	11.11	8.88	7.85	7.62	281.2	155.5	112.1	68.9	9.14	1.06	0.259
0.25E-09	0.000443	14.31	11.11	8.88	7.85	7.62	281.3	155.6	112.2	69.0	9.25	1.07	0.262
0.50E-09	0.000886	14.31	11.11	8.88	7.85	7.62	281.4	155.8	112.4	69.3	9.45	1.08	0.266
0.10E-08	0.001772	14.31	11.11	8.88	7.85	7.62	281.7	156.1	112.7	69.7	9.84	1.12	0.276
0.25E-08	0.004427	14.32	11.11	8.88	7.85	7.62	282.7	157.1	113.6	71.1	11.01	1.22	0.305
0.50E-08	0.008850	14.33	11.12	8.88	7.85	7.62	284.2	158.7	115.2	73.4	12.96	1.38	0.353
0.10E-07	0.017680	14.36	11.13	8.89	7.86	7.62	287.4	162.0	118.3	78.0	16.84	1.71	0.449
0.25E-07	0.044059	14.43	11.17	8.91	7.87	7.61	296.6	171.7	127.6	91.7	28.38	2.71	0.736
0.50E-07	0.087653	14.56	11.24	8.94	7.88	7.61	311.6	187.5	142.7	113.8	47.24	4.34	1.208
0.10E-06	0.173581	14.80	11.37	9.01	7.91	7.60	339.6	217.3	171.5	155.1	83.19	7.52	2.134
0.25E-06	0.422370	15.50	11.74	9.19	8.01	7.59	414.1	298.5	250.7	265.0	182.33	16.60	4.808
0.50E-06	0.812462	16.59	12.33	9.49	8.16	7.60	513.3	412.2	364.4	413.1	326.14	30.85	9.054
0.10E-05	1.529354	18.55	13.41	10.04	8.47	7.67	648.7	583.4	544.2	628.4	561.40	57.22	17.049
0.20E-05	2.807379	21.91	15.32	11.04	9.05	7.89	783.8	797.9	793.6	898.7	923.12	106.43	32.235
0.40E-05	5.023285	27.32	18.55	12.76	10.10	8.39	837.4	993.4	1079.0	1188.5	1463.73	200.89	61.868
0.60E-05	6.980643	31.68	21.31	14.22	10.99	8.87	798.9	1059.0	1231.1	1347.7	1895.70	293.94	91.423
0.10E-04	10.448120	38.24	25.77	16.58	12.46	9.70	674.0	1055.7	1364.5	1513.5	2593.55	476.13	149.974
0.20E-04	17.651398	46.96	32.24	20.26	14.86	11.19	439.2	898.6	1386.7	1625.8	3805.07	904.41	290.438

Table A.10. Optical, NIR, IRAC and MIPS magnitudes and fluxes for a O-rich AGB star, $T_{\text{eff}} = 2500$ K, 60% Silicate + 40% Alox.

\bar{M}	τ	V	I	J	H	K	3.6	4.5	5.8	8.0	24	70	160
0.10E-09	0.000189	17.04	12.72	8.67	7.87	7.44	451.6	318.1	247.5	153.0	24.18	2.86	0.704
0.25E-09	0.000473	17.04	12.72	8.67	7.87	7.44	451.7	318.2	247.6	153.1	24.29	2.87	0.706
0.50E-09	0.000945	17.04	12.72	8.67	7.87	7.44	451.8	318.3	247.7	153.3	24.46	2.88	0.711
0.10E-08	0.001890	17.04	12.72	8.67	7.87	7.44	452.0	318.5	248.0	153.7	24.80	2.91	0.719
0.25E-08	0.004724	17.05	12.73	8.68	7.87	7.44	452.7	319.3	248.7	154.8	25.84	3.00	0.746
0.50E-08	0.009443	17.07	12.73	8.68	7.87	7.44	453.9	320.6	250.0	156.8	27.57	3.15	0.789
0.10E-07	0.018867	17.09	12.74	8.69	7.88	7.44	456.1	323.1	252.5	160.7	31.01	3.45	0.877
0.25E-07	0.047024	17.17	12.78	8.71	7.89	7.44	462.9	330.7	260.1	172.2	41.29	4.36	1.139
0.50E-07	0.093601	17.30	12.85	8.75	7.91	7.44	473.9	343.2	272.5	191.1	58.21	5.85	1.575
0.10E-06	0.185460	17.55	12.97	8.82	7.94	7.45	494.9	367.2	296.6	226.8	90.86	8.80	2.435
0.25E-06	0.451768	18.28	13.34	9.03	8.05	7.47	552.1	434.2	364.4	324.2	183.13	17.43	4.977
0.50E-06	0.870331	19.41	13.92	9.36	8.23	7.51	629.8	530.3	464.4	458.7	320.22	31.25	9.092
0.10E-05	1.638781	21.42	14.99	9.98	8.56	7.62	737.1	678.7	627.1	660.0	550.79	57.47	17.022
0.20E-05	3.002760	24.73	16.88	11.06	9.17	7.88	839.2	866.0	856.8	918.9	914.01	107.32	32.366
0.40E-05	5.350884	29.73	20.03	12.89	10.25	8.42	860.2	1032.6	1121.6	1202.7	1467.29	204.21	62.716
0.60E-05	7.411087	33.51	22.61	14.41	11.16	8.92	806.5	1082.5	1262.0	1360.1	1912.58	300.16	93.173
0.10E-04	11.034332	39.04	26.55	16.79	12.61	9.77	670.1	1063.4	1382.5	1523.5	2630.71	488.75	153.809
0.20E-04	18.517899	47.33	32.52	20.44	14.98	11.26	430.1	892.0	1388.0	1630.4	3866.10	928.97	298.269

Table A.11. Optical, NIR, IRAC and MIPS magnitudes and fluxes for a O-rich AGB star, $T_{\text{eff}} = 3850$ K, 100% Silicate.

\bar{M}	τ	V	I	J	H	K	3.6	4.5	5.8	8.0	24	70	160
0.10E-09	0.000113	11.84	10.19	9.08	8.21	8.08	177.4	98.4	69.8	42.2	5.37	0.61	0.150
0.25E-09	0.000283	11.84	10.19	9.08	8.21	8.08	177.4	98.4	69.9	42.4	5.50	0.62	0.153
0.50E-09	0.000566	11.84	10.19	9.08	8.21	8.08	177.5	98.6	70.0	42.6	5.71	0.64	0.158
0.10E-08	0.001132	11.84	10.19	9.09	8.21	8.08	177.7	98.8	70.3	43.1	6.14	0.67	0.167
0.25E-08	0.002830	11.84	10.19	9.09	8.21	8.08	178.3	99.6	71.1	44.5	7.42	0.76	0.196
0.50E-08	0.005659	11.85	10.19	9.09	8.21	8.08	179.3	100.9	72.5	46.8	9.55	0.92	0.245
0.10E-07	0.011312	11.86	10.20	9.09	8.21	8.08	181.3	103.5	75.4	51.4	13.80	1.23	0.341
0.25E-07	0.028240	11.88	10.21	9.10	8.22	8.08	187.2	111.1	83.7	65.2	26.46	2.16	0.628
0.50E-07	0.056346	11.93	10.24	9.12	8.23	8.08	196.8	123.7	97.5	87.8	47.27	3.70	1.101
0.10E-06	0.112164	12.01	10.30	9.15	8.25	8.08	215.5	148.3	124.5	131.6	87.88	6.70	2.032
0.25E-06	0.276816	12.26	10.46	9.25	8.31	8.09	265.6	215.0	198.5	248.9	201.40	15.28	4.711
0.50E-06	0.543087	12.67	10.71	9.40	8.42	8.11	335.9	311.6	307.5	413.6	370.06	28.41	8.865
0.10E-05	1.051946	13.45	11.21	9.70	8.62	8.17	440.0	463.2	484.4	661.2	653.45	51.92	16.413
0.20E-05	2.005341	14.89	12.13	10.27	9.00	8.33	556.4	659.9	733.4	973.3	1090.65	92.79	29.768
0.40E-05	3.758634	17.51	13.81	11.31	9.73	8.73	622.0	844.4	1019.0	1293.2	1720.34	165.01	53.695
0.60E-05	5.383984	19.89	15.36	12.27	10.41	9.14	602.6	904.2	1167.4	1458.2	2198.09	232.86	76.317
0.10E-04	8.390248	24.19	18.20	14.04	11.67	9.94	504.1	889.2	1286.9	1621.6	2939.84	364.41	120.349
0.20E-04	15.035424	33.23	24.38	17.92	14.41	11.69	292.8	697.5	1252.7	1717.0	4211.82	680.47	226.700

Table A.12. Optical, NIR, IRAC and MIPS magnitudes and fluxes for a O-rich AGB star, $T_{\text{eff}} = 3297$ K, 100% Silicate.

\dot{M}	τ	V	I	J	H	K	3.6	4.5	5.8	8.0	24	70	160
0.10E-09	0.000134	14.31	11.11	8.88	7.85	7.62	281.1	155.5	112.1	68.9	9.13	1.05	0.258
0.25E-09	0.000334	14.31	11.11	8.88	7.85	7.62	281.2	155.5	112.2	69.0	9.24	1.06	0.261
0.50E-09	0.000668	14.31	11.11	8.88	7.85	7.62	281.3	155.7	112.3	69.2	9.42	1.07	0.265
0.10E-08	0.001337	14.31	11.11	8.88	7.85	7.62	281.4	155.9	112.5	69.6	9.78	1.10	0.273
0.25E-08	0.003342	14.31	11.11	8.88	7.85	7.62	281.8	156.5	113.2	70.7	10.86	1.18	0.298
0.50E-08	0.006681	14.32	11.11	8.88	7.85	7.62	282.6	157.5	114.4	72.7	12.66	1.31	0.338
0.10E-07	0.013355	14.33	11.12	8.89	7.86	7.62	284.1	159.6	116.7	76.6	16.25	1.58	0.420
0.25E-07	0.033331	14.36	11.14	8.90	7.86	7.63	288.5	165.9	123.7	88.2	27.01	2.37	0.664
0.50E-07	0.066475	14.41	11.17	8.92	7.88	7.63	295.7	176.2	135.2	107.3	44.80	3.69	1.070
0.10E-06	0.132220	14.52	11.23	8.96	7.90	7.64	309.9	196.6	158.0	144.6	79.94	6.30	1.877
0.25E-06	0.325542	14.82	11.42	9.07	7.98	7.68	348.7	253.0	221.9	246.4	180.15	13.92	4.244
0.50E-06	0.636353	15.31	11.71	9.25	8.11	7.74	405.3	338.1	320.0	394.7	335.42	26.09	8.059
0.10E-05	1.224941	16.23	12.27	9.60	8.35	7.86	491.7	477.5	486.8	628.4	608.28	48.84	15.280
0.20E-05	2.312776	17.90	13.31	10.25	8.80	8.11	591.5	668.7	734.9	941.4	1047.89	89.93	28.543
0.40E-05	4.274016	20.87	15.16	11.41	9.62	8.59	642.5	854.4	1029.7	1278.9	1691.05	163.33	52.621
0.60E-05	6.058981	23.51	16.83	12.46	10.37	9.06	614.6	914.0	1182.9	1455.1	2175.69	231.93	75.330
0.10E-04	9.300130	28.12	19.84	14.36	11.73	9.92	506.7	894.9	1301.6	1626.3	2922.00	364.24	119.400
0.20E-04	16.298681	37.43	26.26	18.42	14.58	11.74	289.9	695.7	1256.4	1719.5	4197.20	680.74	225.611

Table A.13. Optical, NIR, IRAC and MIPS magnitudes and fluxes for a O-rich AGB star, $T_{\text{eff}} = 2500$ K, 100% Silicate.

\dot{M}	τ	V	I	J	H	K	3.6	4.5	5.8	8.0	24	70	160
0.10E-09	0.000144	17.04	12.72	8.67	7.87	7.44	451.6	318.1	247.5	153.0	24.18	2.85	0.703
0.25E-09	0.000361	17.04	12.72	8.67	7.87	7.44	451.6	318.1	247.6	153.1	24.28	2.86	0.706
0.50E-09	0.000722	17.04	12.72	8.67	7.87	7.44	451.7	318.2	247.7	153.2	24.44	2.87	0.709
0.10E-08	0.001445	17.04	12.72	8.67	7.87	7.44	451.8	318.4	247.9	153.6	24.77	2.90	0.717
0.25E-08	0.003611	17.05	12.72	8.67	7.87	7.44	452.1	318.9	248.5	154.6	25.76	2.97	0.739
0.50E-08	0.007219	17.05	12.73	8.68	7.87	7.44	452.6	319.7	249.5	156.4	27.40	3.09	0.777
0.10E-07	0.014430	17.06	12.73	8.68	7.88	7.44	453.7	321.4	251.5	159.8	30.69	3.34	0.852
0.25E-07	0.036011	17.10	12.75	8.69	7.89	7.45	456.9	326.6	257.4	170.2	40.54	4.07	1.078
0.50E-07	0.071808	17.15	12.79	8.72	7.90	7.45	462.1	335.0	267.3	187.2	56.88	5.29	1.454
0.10E-06	0.142781	17.27	12.85	8.76	7.93	7.47	472.4	351.8	287.0	220.5	89.31	7.72	2.205
0.25E-06	0.351215	17.59	13.05	8.88	8.01	7.52	500.6	398.7	342.9	312.4	182.55	14.86	4.424
0.50E-06	0.685568	18.12	13.36	9.08	8.15	7.59	542.2	470.5	429.8	447.9	329.21	26.46	8.050
0.10E-05	1.316403	19.10	13.95	9.45	8.41	7.74	605.3	589.7	580.4	664.9	591.54	48.52	15.029
0.20E-05	2.475791	20.88	15.03	10.14	8.89	8.02	673.4	753.7	807.8	961.3	1022.64	89.15	28.088
0.40E-05	4.548722	23.99	16.96	11.37	9.75	8.55	688.1	908.0	1079.7	1288.8	1665.93	162.90	52.182
0.60E-05	6.420008	26.71	18.68	12.47	10.53	9.04	640.9	949.6	1219.8	1463.3	2156.55	232.28	75.076
0.10E-04	9.786523	31.38	21.77	14.45	11.92	9.95	515.3	911.5	1323.5	1634.8	2914.18	365.78	119.425
0.20E-04	16.987080	40.68	28.28	18.62	14.79	11.79	289.4	698.3	1264.4	1726.4	4206.51	685.39	226.565

Table A.14. ASTRO-F fluxes for a C-rich AGB star, $T_{\text{eff}} = 2650$ K, 85% AMC + 15% SiC.

\dot{M}	τ	IRC_N2	IRC_N3	IRC_N4	S7	S9W	S11	L15	L18W	L24	N60	WIDE-S	WIDE-L	N160
0.10E-09	0.000045	637.4	296.2	255.2	90.4	65.8	39.5	25.3	21.1	23.7	3.40	2.26	0.83	0.66
0.25E-09	0.000113	637.5	296.4	255.5	90.6	66.0	39.7	25.4	21.1	23.7	3.41	2.27	0.83	0.67
0.50E-09	0.000226	637.6	296.7	255.9	91.0	66.4	40.1	25.5	21.3	23.8	3.43	2.28	0.84	0.67
0.10E-08	0.000452	637.8	297.3	256.7	91.8	67.3	40.8	25.9	21.5	24.0	3.47	2.31	0.85	0.68
0.25E-08	0.001130	638.5	299.2	259.2	94.3	69.9	42.9	27.0	22.2	24.6	3.60	2.40	0.88	0.70
0.50E-08	0.002259	639.7	302.4	263.4	98.3	74.1	46.3	28.8	23.4	25.6	3.80	2.54	0.93	0.74
0.10E-07	0.004513	642.0	308.6	271.7	106.4	82.6	53.2	32.3	25.8	27.5	4.21	2.83	1.03	0.81
0.25E-07	0.011247	648.5	326.8	296.2	130.1	107.7	73.7	42.9	32.7	33.2	5.44	3.70	1.33	1.04
0.50E-07	0.022382	658.4	355.8	335.5	168.7	148.3	106.8	60.0	44.0	42.5	7.43	5.10	1.82	1.41
0.10E-06	0.044342	674.1	407.8	408.2	241.3	225.1	169.5	92.6	65.6	60.3	11.23	7.78	2.76	2.12
0.25E-06	0.108009	699.4	531.6	591.7	433.0	428.1	335.4	180.4	123.9	108.3	21.54	15.06	5.31	4.04
0.50E-06	0.208266	696.0	661.2	813.9	688.6	700.4	559.0	303.0	205.5	175.9	36.20	25.40	8.95	6.78
0.10E-05	0.393236	620.3	766.7	1076.8	1059.3	1100.9	891.5	498.8	337.1	285.6	60.38	42.49	14.95	11.30
0.20E-05	0.725089	437.3	748.9	1276.4	1526.8	1625.1	1339.1	802.5	545.4	462.5	100.53	70.92	24.98	18.86
0.40E-05	1.306390	208.7	553.7	1266.6	2014.1	2224.6	1884.9	1275.1	881.0	757.0	170.69	120.81	42.69	32.23
0.60E-05	1.825759	106.4	391.9	1130.8	2244.5	2560.6	2223.2	1661.7	1166.5	1016.9	235.93	167.38	59.34	44.82
0.10E-04	2.756648	34.3	207.2	856.3	2392.6	2887.3	2614.6	2287.2	1650.3	1477.1	358.97	255.66	91.18	68.94

Table A.15. ASTRO-F fluxes for a C-rich AGB star, $T_{\text{eff}} = 3600$ K, 85% AMC + 15% SiC.

\dot{M}	τ	IRC_N2	IRC_N3	IRC_N4	S7	S9W	S11	L15	L18W	L24	N60	WIDE-S	WIDE-L	N160
0.10E-09	0.000040	404.9	262.9	160.5	78.4	57.1	33.6	19.7	12.5	8.7	1.17	0.77	0.28	0.23
0.25E-09	0.000099	405.0	263.1	160.8	78.7	57.4	33.9	19.9	12.6	8.8	1.18	0.78	0.29	0.23
0.50E-09	0.000198	405.3	263.5	161.3	79.2	57.9	34.3	20.1	12.7	8.9	1.21	0.80	0.29	0.23
0.10E-08	0.000395	405.7	264.3	162.3	80.1	58.9	35.1	20.5	13.0	9.1	1.25	0.84	0.30	0.24
0.25E-08	0.000988	407.1	266.6	165.3	82.9	61.8	37.5	21.7	13.8	9.8	1.40	0.94	0.34	0.27
0.50E-08	0.001975	409.4	270.4	170.3	87.6	66.8	41.5	23.8	15.2	10.9	1.64	1.10	0.40	0.31
0.10E-07	0.003946	413.9	278.0	180.2	96.9	76.6	49.5	27.9	17.9	13.2	2.11	1.44	0.51	0.40
0.25E-07	0.009838	427.0	300.1	209.3	124.2	105.3	72.8	39.9	25.8	19.7	3.50	2.42	0.86	0.66
0.50E-07	0.019587	447.1	334.8	255.6	168.0	151.3	110.3	59.2	38.6	30.2	5.75	4.01	1.42	1.08
0.10E-06	0.038832	481.9	397.5	340.6	249.3	236.8	179.8	95.2	62.4	49.8	9.96	6.99	2.47	1.87
0.25E-06	0.094927	548.4	538.7	545.7	455.1	454.4	357.5	189.0	124.6	101.1	20.93	14.71	5.17	3.91
0.50E-06	0.184005	590.5	680.7	783.0	715.6	731.3	584.6	313.0	207.2	169.5	35.76	25.18	8.84	6.67
0.10E-05	0.350641	564.6	790.9	1052.7	1077.8	1122.6	909.7	504.2	335.8	277.1	59.54	41.99	14.76	11.14
0.20E-05	0.655079	422.2	771.7	1256.6	1528.4	1629.8	1344.0	799.3	538.6	449.9	98.94	69.91	24.62	18.56
0.40E-05	1.199514	211.5	572.0	1259.4	2007.2	2220.6	1883.0	1264.8	869.7	741.3	168.54	119.43	42.22	31.85
0.60E-05	1.693328	110.2	405.8	1132.8	2239.9	2557.5	2221.3	1648.0	1152.8	999.4	233.30	165.69	58.76	44.36
0.10E-04	2.589452	36.1	214.8	865.3	2395.9	2890.0	2615.6	2270.2	1633.5	1456.7	355.30	253.25	90.37	68.31

Table A.16. ASTRO-F fluxes for a C-rich AGB star, $T_{\text{eff}} = 2650$ K, 100% AMC.

\dot{M}	τ	IRC_N2	IRC_N3	IRC_N4	S7	S9W	S11	L15	L18W	L24	N60	WIDE-S	WIDE-L	N160
0.10E-09	0.000017	637.4	296.2	255.2	90.4	65.8	39.5	25.3	21.1	23.7	3.40	2.26	0.83	0.66
0.25E-09	0.000043	637.5	296.4	255.5	90.7	66.0	39.6	25.4	21.2	23.7	3.41	2.27	0.83	0.67
0.50E-09	0.000086	637.6	296.7	256.0	91.2	66.4	39.9	25.6	21.3	23.8	3.44	2.29	0.84	0.67
0.10E-08	0.000172	637.9	297.4	256.9	92.1	67.2	40.5	25.9	21.6	24.1	3.49	2.33	0.86	0.69
0.25E-08	0.000429	638.6	299.4	259.6	95.0	69.7	42.1	27.1	22.3	24.7	3.64	2.44	0.91	0.73
0.50E-08	0.000857	639.9	302.7	264.2	99.7	73.8	44.9	28.9	23.6	25.8	3.90	2.64	0.99	0.79
0.10E-07	0.001712	642.3	309.3	273.3	109.1	81.9	50.4	32.7	26.2	28.0	4.40	3.02	1.15	0.92
0.25E-07	0.004267	649.3	328.6	299.9	136.8	105.8	66.7	43.7	33.9	34.4	5.90	4.15	1.63	1.31
0.50E-07	0.008490	659.9	359.1	342.7	181.6	144.5	93.0	61.6	46.3	44.8	8.32	5.98	2.42	1.94
0.10E-06	0.016815	676.5	413.7	421.2	265.7	217.4	142.9	95.5	69.9	64.6	12.95	9.48	3.92	3.16
0.25E-06	0.040938	703.0	541.8	617.0	484.7	408.9	274.6	186.1	133.0	117.6	25.38	18.89	7.99	6.46
0.50E-06	0.078906	698.6	672.8	848.9	771.4	664.3	453.3	311.4	220.5	191.4	42.86	32.14	13.80	11.21
0.10E-05	0.148964	619.7	774.6	1115.1	1177.8	1041.2	726.1	511.1	360.8	310.5	71.54	53.93	23.46	19.15
0.20E-05	0.274773	433.5	748.5	1305.4	1676.8	1546.0	1117.4	823.8	583.7	503.0	119.17	90.19	39.66	32.53
0.40E-05	0.495402	205.6	546.9	1274.5	2172.3	2148.5	1645.9	1316.2	943.8	823.2	201.93	153.32	68.00	56.01
0.60E-05	0.692600	104.8	384.4	1124.7	2384.2	2501.4	2008.0	1719.5	1247.3	1102.3	277.54	211.13	94.04	77.60
0.10E-04	1.046017	33.9	201.4	836.1	2475.5	2862.5	2471.6	2366.0	1752.2	1586.1	416.61	317.77	142.24	117.59

Table A.17. ASTRO-F fluxes for a C-rich AGB star, $T_{\text{eff}} = 3600$ K, 100% AMC.

\dot{M}	τ	IRC_N2	IRC_N3	IRC_N4	S7	S9W	S11	L15	L18W	L24	N60	WIDE-S	WIDE-L	N160
0.10E-09	0.000015	404.9	262.9	160.5	78.5	57.1	33.6	19.8	12.5	8.7	1.17	0.78	0.28	0.23
0.25E-09	0.000037	405.0	263.2	160.8	78.8	57.4	33.8	19.9	12.6	8.8	1.19	0.79	0.29	0.23
0.50E-09	0.000074	405.3	263.6	161.4	79.3	57.8	34.1	20.1	12.7	9.0	1.22	0.81	0.30	0.24
0.10E-08	0.000149	405.8	264.4	162.5	80.5	58.8	34.8	20.5	13.0	9.2	1.28	0.86	0.32	0.26
0.25E-08	0.000372	407.3	266.9	165.8	83.8	61.7	36.7	21.9	14.0	10.0	1.45	0.99	0.38	0.30
0.50E-08	0.000743	409.7	271.0	171.3	89.3	66.4	39.9	24.0	15.5	11.2	1.75	1.21	0.47	0.38
0.10E-07	0.001485	414.5	279.0	182.2	100.2	75.8	46.3	28.4	18.5	13.8	2.33	1.65	0.66	0.53
0.25E-07	0.003703	428.3	302.5	214.1	132.3	103.4	65.0	41.0	27.3	21.1	4.05	2.95	1.21	0.97
0.50E-07	0.007372	449.5	339.3	264.6	183.4	147.4	94.9	61.2	41.3	32.9	6.79	5.02	2.10	1.69
0.10E-06	0.014614	485.7	405.1	356.6	277.6	228.7	150.2	98.7	67.4	54.8	11.89	8.88	3.76	3.04
0.25E-06	0.035722	554.0	551.3	575.4	513.0	434.0	291.3	195.5	134.7	111.4	25.15	18.93	8.13	6.59
0.50E-06	0.069241	595.2	694.4	822.2	804.1	692.5	471.7	321.7	222.9	185.8	42.78	32.30	14.02	11.42
0.10E-05	0.132019	565.5	799.8	1093.7	1199.5	1059.0	737.0	516.0	359.7	302.2	70.89	53.67	23.54	19.27
0.20E-05	0.246947	419.3	771.5	1287.7	1679.7	1546.3	1115.6	819.6	576.6	490.3	117.67	89.30	39.49	32.47
0.40E-05	0.452970	208.7	565.2	1269.7	2167.9	2139.7	1636.1	1304.5	931.8	807.2	199.81	152.01	67.68	55.82
0.60E-05	0.640216	108.6	398.2	1128.8	2383.7	2494.0	1997.5	1704.5	1233.2	1084.6	274.96	209.50	93.59	77.30
0.10E-04	0.979777	35.7	208.9	846.5	2483.9	2861.5	2463.8	2347.5	1735.0	1565.4	412.84	315.24	141.40	116.97

Table A.18. ASTRO-F fluxes for a O-rich AGB star, $T_{\text{eff}} = 3850$ K, 100% AlOx.

\dot{M}	τ	IRC_N2	IRC_N3	IRC_N4	S7	S9W	S11	L15	L18W	L24	N60	WIDE-S	WIDE-L	N160
0.10E-09	0.000200	360.6	198.0	115.6	54.7	38.3	21.7	12.5	7.9	5.5	0.72	0.48	0.16	0.13
0.25E-09	0.000499	360.6	198.1	115.7	54.8	38.5	22.0	12.9	8.1	5.6	0.73	0.48	0.17	0.13
0.50E-09	0.000998	360.6	198.1	115.7	54.9	38.8	22.5	13.4	8.4	5.8	0.75	0.50	0.17	0.13
0.10E-08	0.001996	360.7	198.2	115.8	55.1	39.5	23.4	14.6	9.0	6.1	0.79	0.53	0.18	0.14
0.25E-08	0.004989	360.9	198.4	116.0	55.8	41.4	26.3	17.9	11.0	7.1	0.91	0.61	0.21	0.17
0.50E-08	0.009974	361.2	198.7	116.5	56.9	44.7	31.1	23.5	14.1	8.8	1.10	0.75	0.27	0.21
0.10E-07	0.019932	361.9	199.4	117.3	59.1	51.1	40.6	34.6	20.5	12.1	1.49	1.04	0.37	0.29
0.25E-07	0.049715	363.9	201.5	119.9	65.7	70.3	68.6	67.4	39.2	22.0	2.66	1.88	0.69	0.53
0.50E-07	0.099054	367.1	205.0	124.3	76.7	101.4	113.4	120.2	69.6	38.5	4.62	3.30	1.23	0.94
0.10E-06	0.196662	373.7	212.1	133.0	98.5	160.4	196.6	219.1	127.5	70.8	8.53	6.14	2.30	1.75
0.25E-06	0.482194	392.7	232.6	158.3	160.7	311.0	397.5	463.4	276.8	161.2	20.03	14.48	5.45	4.16
0.50E-06	0.938610	422.3	265.5	199.4	257.9	505.7	631.3	759.5	472.5	296.7	38.78	28.11	10.64	8.12
0.10E-05	1.801754	472.8	325.2	275.0	425.7	759.5	885.2	1107.8	735.5	518.6	74.43	54.13	20.65	15.80
0.20E-05	3.412976	541.7	421.2	402.9	678.5	1011.8	1055.5	1398.7	1017.8	834.5	139.53	101.98	39.34	30.23
0.40E-05	6.387136	598.9	548.2	591.6	982.1	1170.1	1057.0	1538.5	1259.2	1222.7	254.89	187.74	73.54	56.82
0.60E-05	9.165066	600.9	622.6	723.7	1145.6	1197.9	987.2	1557.1	1379.3	1480.8	360.56	267.22	105.82	82.03
0.10E-04	14.355180	545.6	691.3	893.7	1299.0	1177.2	866.9	1552.9	1534.1	1863.1	560.15	419.09	168.51	131.17
0.20E-04	26.049158	375.1	694.8	1078.2	1399.7	1099.2	703.9	1528.5	1780.2	2534.1	1027.55	780.42	320.90	251.12

Table A.19. ASTRO-F fluxes for a O-rich AGB star, $T_{\text{eff}} = 3297$ K, 100% AlOx.

\dot{M}	τ	IRC_N2	IRC_N3	IRC_N4	S7	S9W	S11	L15	L18W	L24	N60	WIDE-S	WIDE-L	N160
0.10E-09	0.000242	525.1	294.4	185.0	89.3	63.1	36.1	21.1	13.4	9.3	1.23	0.82	0.28	0.22
0.25E-09	0.000604	525.1	294.4	185.1	89.3	63.3	36.3	21.4	13.5	9.4	1.24	0.83	0.28	0.22
0.50E-09	0.001209	525.1	294.4	185.1	89.4	63.5	36.7	21.8	13.8	9.6	1.26	0.84	0.29	0.23
0.10E-08	0.002417	525.1	294.5	185.2	89.6	64.1	37.5	22.7	14.3	9.8	1.29	0.86	0.30	0.23
0.25E-08	0.006041	525.2	294.6	185.4	90.1	65.6	39.8	25.5	15.8	10.6	1.39	0.93	0.32	0.25
0.50E-08	0.012076	525.3	294.8	185.7	91.0	68.2	43.6	30.0	18.4	12.0	1.55	1.04	0.37	0.29
0.10E-07	0.024129	525.6	295.3	186.3	92.7	73.4	51.2	38.9	23.5	14.7	1.87	1.28	0.45	0.35
0.25E-07	0.060160	526.4	296.8	188.3	98.0	88.7	73.6	65.3	38.6	22.8	2.83	1.98	0.72	0.55
0.50E-07	0.119790	527.8	299.2	191.6	106.7	113.5	109.4	107.8	63.3	36.3	4.46	3.15	1.16	0.89
0.10E-06	0.237577	530.7	304.2	198.3	124.1	160.0	174.7	186.3	109.6	62.6	7.70	5.50	2.04	1.56
0.25E-06	0.580645	539.9	319.4	218.8	176.0	282.8	336.5	385.7	233.2	139.4	17.65	12.71	4.76	3.62
0.50E-06	1.125672	555.8	345.0	253.3	259.2	443.5	526.0	630.3	398.0	257.1	34.38	24.87	9.36	7.13
0.10E-05	2.149076	585.0	394.3	320.2	409.2	664.3	744.9	936.2	631.5	457.9	67.52	49.04	18.58	14.17
0.20E-05	4.038786	625.6	478.2	439.7	645.6	904.9	919.2	1231.7	908.2	760.3	130.66	95.41	36.51	27.93
0.40E-05	7.465082	649.5	593.5	623.5	940.8	1083.5	965.3	1427.3	1177.4	1155.5	245.90	180.98	70.32	54.06
0.60E-05	10.610692	632.3	661.3	754.1	1103.3	1129.4	923.4	1480.0	1318.6	1425.4	352.35	260.98	102.57	79.14
0.10E-04	16.384277	555.6	720.2	921.1	1260.2	1131.4	831.5	1509.2	1497.0	1825.6	553.67	414.07	165.40	128.22
0.20E-04	29.073149	368.9	707.0	1094.7	1375.8	1080.5	693.6	1515.8	1768.4	2521.0	1023.92	777.25	317.85	247.89

Table A.20. ASTRO-F fluxes for a O-rich AGB star, $T_{\text{eff}} = 2500$ K, 100% AlOx.

\dot{M}	τ	IRC_N2	IRC_N3	IRC_N4	S7	S9W	S11	L15	L18W	L24	N60	WIDE-S	WIDE-L	N160
0.10E-09	0.000258	667.9	458.3	362.0	198.2	143.8	86.4	54.9	35.0	24.8	3.34	2.22	0.77	0.60
0.25E-09	0.000644	667.9	458.3	362.0	198.2	144.0	86.6	55.1	35.1	24.8	3.35	2.22	0.77	0.60
0.50E-09	0.001287	667.9	458.3	362.0	198.3	144.2	86.9	55.5	35.3	24.9	3.36	2.23	0.77	0.61
0.10E-08	0.002575	667.9	458.3	362.1	198.4	144.6	87.5	56.3	35.8	25.2	3.39	2.26	0.78	0.61
0.25E-08	0.006435	667.9	458.4	362.2	198.8	145.9	89.5	58.6	37.1	25.9	3.48	2.32	0.80	0.63
0.50E-08	0.012865	667.9	458.6	362.5	199.5	148.0	92.6	62.4	39.3	27.1	3.62	2.42	0.84	0.66
0.10E-07	0.025708	668.0	458.9	362.9	200.9	152.3	99.0	70.0	43.7	29.4	3.91	2.63	0.92	0.72
0.25E-07	0.064110	668.0	459.8	364.4	205.1	164.8	117.5	92.4	56.6	36.5	4.78	3.26	1.16	0.90
0.50E-07	0.127692	668.2	461.3	366.8	212.2	185.3	147.2	128.5	77.7	48.3	6.25	4.33	1.57	1.21
0.10E-06	0.253438	668.7	464.5	371.8	226.4	223.8	201.6	195.3	117.6	71.5	9.20	6.47	2.38	1.83
0.25E-06	0.620454	671.3	474.8	387.5	269.4	326.0	336.7	366.1	224.9	139.6	18.33	13.11	4.89	3.74
0.50E-06	1.205401	677.2	493.0	414.8	339.8	461.6	496.5	578.5	370.1	245.8	33.91	24.45	9.19	7.02
0.10E-05	2.307303	689.7	529.5	469.7	469.7	651.7	685.3	852.0	581.4	430.7	65.32	47.40	17.95	13.70
0.20E-05	4.345098	704.9	593.6	570.4	678.2	865.2	843.4	1131.3	842.5	716.5	126.38	92.29	35.31	27.02
0.40E-05	8.036496	696.4	681.4	728.2	943.2	1031.8	896.5	1338.2	1113.3	1105.1	240.46	177.07	68.77	52.85
0.60E-05	11.411263	659.0	730.1	840.9	1092.2	1081.7	869.7	1410.8	1266.4	1381.3	347.79	257.77	101.25	78.07
0.10E-04	17.578022	560.8	763.7	983.8	1241.8	1097.1	799.6	1469.3	1466.8	1800.8	553.57	414.24	165.34	128.05
0.20E-04	31.022861	360.8	722.1	1127.4	1363.7	1065.4	681.5	1503.2	1764.3	2528.7	1037.73	788.06	321.99	250.90

Table A.21. ASTRO-F fluxes for a O-rich AGB star, $T_{\text{eff}} = 3850$ K, 60% Silicate + 40% AlOx.

\dot{M}	τ	IRC_N2	IRC_N3	IRC_N4	S7	S9W	S11	L15	L18W	L24	N60	WIDE-S	WIDE-L	N160
0.10E-09	0.000145	360.6	198.1	115.7	54.8	38.5	21.8	12.5	7.9	5.5	0.72	0.48	0.16	0.13
0.25E-09	0.000362	360.7	198.2	115.8	54.9	38.9	22.4	12.9	8.2	5.7	0.73	0.49	0.17	0.13
0.50E-09	0.000725	360.9	198.4	116.1	55.1	39.7	23.3	13.5	8.5	5.9	0.76	0.50	0.17	0.14
0.10E-08	0.001449	361.2	198.8	116.5	55.6	41.3	25.0	14.7	9.3	6.4	0.80	0.54	0.19	0.15
0.25E-08	0.003621	362.2	200.0	117.8	56.9	46.0	30.3	18.3	11.6	7.9	0.95	0.64	0.23	0.18
0.50E-08	0.007239	363.9	201.9	120.0	59.1	53.8	39.0	24.3	15.4	10.4	1.18	0.81	0.29	0.23
0.10E-07	0.014465	367.1	205.8	124.4	63.6	69.2	56.3	36.1	23.0	15.4	1.65	1.14	0.42	0.33
0.25E-07	0.036064	376.6	217.2	137.4	76.6	114.0	106.5	70.9	45.3	29.9	3.02	2.12	0.80	0.62
0.50E-07	0.071808	391.6	235.5	158.1	97.6	184.3	185.1	126.2	80.8	53.4	5.24	3.71	1.41	1.11
0.10E-06	0.142381	418.7	269.3	197.2	137.3	310.1	325.7	228.3	146.9	97.4	9.44	6.73	2.58	2.03
0.25E-06	0.348180	479.3	350.9	294.5	238.0	586.0	631.8	474.2	309.8	210.9	20.94	15.00	5.83	4.59
0.50E-06	0.675066	540.7	449.5	420.7	373.8	868.8	938.8	770.6	514.6	364.2	37.66	27.06	10.63	8.40
0.10E-05	1.287621	586.1	568.3	597.1	579.5	1142.8	1216.9	1149.2	797.1	602.9	67.51	48.65	19.31	15.34
0.20E-05	2.408700	563.4	667.3	807.4	867.2	1341.3	1374.7	1573.1	1156.2	962.7	122.65	88.71	35.59	28.40
0.40E-05	4.416763	432.3	677.7	994.3	1225.9	1456.1	1399.6	2021.5	1603.4	1499.1	228.73	166.15	67.32	53.93
0.60E-05	6.234009	319.7	621.0	1054.1	1445.4	1489.4	1366.8	2295.8	1917.0	1925.3	333.02	242.67	98.88	79.37
0.10E-04	9.513249	182.7	492.7	1044.2	1692.3	1490.8	1283.4	2642.0	2369.8	2610.7	537.86	393.83	161.69	130.08
0.20E-04	16.500765	63.4	289.3	876.9	1894.5	1398.8	1091.1	3019.4	3031.4	3805.3	1023.21	755.68	313.97	253.34

Table A.22. ASTRO-F fluxes for a O-rich AGB star, $T_{\text{eff}} = 3297$ K, 60% Silicate + 40% AlOx.

\dot{M}	τ	IRC_N2	IRC_N3	IRC_N4	S7	S9W	S11	L15	L18W	L24	N60	WIDE-S	WIDE-L	N160
0.10E-09	0.000177	525.1	294.4	185.1	89.3	63.3	36.2	21.1	13.4	9.4	1.23	0.82	0.28	0.22
0.25E-09	0.000443	525.1	294.5	185.2	89.4	63.6	36.7	21.4	13.6	9.5	1.25	0.83	0.29	0.22
0.50E-09	0.000886	525.2	294.7	185.4	89.6	64.3	37.4	21.9	13.9	9.7	1.27	0.84	0.29	0.23
0.10E-08	0.001772	525.4	294.9	185.7	90.0	65.5	38.8	22.9	14.5	10.1	1.30	0.87	0.30	0.24
0.25E-08	0.004427	525.9	295.8	186.7	91.0	69.3	43.0	25.8	16.3	11.3	1.42	0.95	0.33	0.26
0.50E-08	0.008850	526.8	297.2	188.4	92.8	75.5	50.0	30.6	19.4	13.3	1.61	1.09	0.39	0.30
0.10E-07	0.017680	528.4	299.9	191.8	96.3	87.8	63.8	40.1	25.6	17.3	1.99	1.36	0.49	0.38
0.25E-07	0.044059	533.4	308.1	201.8	106.7	123.8	104.3	68.4	43.7	29.3	3.12	2.17	0.80	0.63
0.50E-07	0.087653	541.2	321.4	218.1	123.8	180.8	168.2	114.0	73.1	48.8	4.99	3.51	1.32	1.03
0.10E-06	0.173581	555.1	346.0	248.8	156.2	282.1	281.5	198.4	128.1	85.9	8.62	6.12	2.33	1.83
0.25E-06	0.422370	587.5	410.4	332.1	245.8	522.6	548.4	417.3	273.8	188.2	19.01	13.58	5.24	4.12
0.50E-06	0.812462	619.1	493.7	448.0	374.8	786.8	834.9	699.0	469.5	336.0	35.28	25.29	9.86	7.77
0.10E-05	1.529354	632.5	600.2	620.5	581.5	1069.9	1123.0	1080.6	754.0	576.5	65.35	47.02	18.52	14.65
0.20E-05	2.807379	580.3	688.9	831.7	876.4	1298.3	1314.3	1522.6	1124.4	943.4	121.36	87.65	34.91	27.76
0.40E-05	5.023285	429.5	686.7	1014.0	1238.0	1437.0	1368.6	1991.3	1583.9	1486.9	228.54	165.85	66.83	53.38
0.60E-05	6.980643	312.8	622.8	1067.0	1455.2	1477.6	1346.8	2276.0	1904.5	1918.2	333.80	243.05	98.61	78.96
0.10E-04	10.448120	176.8	488.5	1045.9	1695.2	1486.4	1276.8	2636.5	2367.1	2610.6	539.25	394.64	161.50	129.69
0.20E-04	17.651398	62.1	286.3	872.3	1888.2	1397.1	1092.4	3019.5	3029.5	3800.0	1019.62	752.77	312.13	251.55

Table A.23. ASTRO-F fluxes for a O-rich AGB star, $T_{\text{eff}} = 2500$ K, 60% Silicate + 40% AlOx.

\dot{M}	τ	IRC_N2	IRC_N3	IRC_N4	S7	S9W	S11	L15	L18W	L24	N60	WIDE-S	WIDE-L	N160
0.10E-09	0.000189	667.9	458.3	362.0	198.2	144.0	86.5	54.9	35.0	24.8	3.34	2.22	0.77	0.60
0.25E-09	0.000473	668.0	458.4	362.1	198.3	144.3	86.9	55.2	35.2	24.9	3.35	2.23	0.77	0.60
0.50E-09	0.000945	668.0	458.5	362.2	198.4	144.8	87.5	55.6	35.4	25.1	3.37	2.24	0.77	0.61
0.10E-08	0.001890	668.1	458.7	362.5	198.7	145.9	88.7	56.4	36.0	25.4	3.40	2.26	0.78	0.62
0.25E-08	0.004724	668.3	459.2	363.3	199.6	149.1	92.3	58.9	37.6	26.5	3.51	2.34	0.81	0.64
0.50E-08	0.009443	668.6	460.2	364.6	201.1	154.3	98.2	63.1	40.3	28.3	3.68	2.46	0.86	0.68
0.10E-07	0.018867	669.3	462.1	367.2	204.0	164.8	110.1	71.5	45.7	31.8	4.02	2.71	0.96	0.75
0.25E-07	0.047024	671.3	467.7	374.9	212.8	195.6	144.8	96.2	61.7	42.5	5.05	3.45	1.24	0.97
0.50E-07	0.093601	674.4	476.9	387.5	227.2	244.4	199.9	136.4	87.7	60.0	6.76	4.68	1.72	1.35
0.10E-06	0.185460	679.9	494.4	411.9	255.0	332.3	298.6	211.7	137.1	93.7	10.13	7.10	2.66	2.08
0.25E-06	0.451768	691.6	541.0	479.6	333.8	545.0	536.0	411.4	271.0	188.8	20.00	14.19	5.43	4.26
0.50E-06	0.870331	698.0	602.1	576.1	450.4	784.9	797.5	675.0	455.5	329.6	35.77	25.56	9.90	7.80
0.10E-05	1.638781	680.0	679.3	723.3	642.4	1052.8	1072.8	1044.4	732.3	565.2	65.66	47.16	18.50	14.62
0.20E-05	3.002760	596.4	734.6	904.1	922.2	1281.6	1271.5	1489.1	1104.4	933.7	122.38	88.32	35.08	27.85
0.40E-05	5.350884	425.0	701.6	1054.4	1270.4	1430.1	1345.4	1977.4	1578.7	1490.0	232.29	168.54	67.78	54.08
0.60E-05	7.411087	304.2	624.9	1090.3	1481.0	1475.6	1333.6	2276.8	1911.8	1934.7	340.82	248.17	100.55	80.44
0.10E-04	11.034332	169.5	482.6	1052.8	1714.2	1484.7	1267.2	2648.2	2387.8	2647.1	553.44	405.13	165.68	132.97
0.20E-04	18.517899	58.9	278.9	865.2	1896.2	1394.5	1086.1	3037.5	3061.7	3859.7	1047.08	773.33	320.60	258.28

Table A.24. ASTRO-F fluxes for a O-rich AGB star, $T_{\text{eff}} = 3850$ K, 100% Silicate.

\dot{M}	τ	IRC_N2	IRC_N3	IRC_N4	S7	S9W	S11	L15	L18W	L24	N60	WIDE-S	WIDE-L	N160
0.10E-09	0.000113	360.6	198.0	115.7	54.8	38.4	21.8	12.4	7.9	5.5	0.72	0.48	0.16	0.13
0.25E-09	0.000283	360.6	198.1	115.7	54.9	38.8	22.2	12.6	8.0	5.6	0.73	0.48	0.17	0.13
0.50E-09	0.000566	360.6	198.2	115.9	55.0	39.5	22.9	13.0	8.3	5.9	0.75	0.50	0.17	0.14
0.10E-08	0.001132	360.7	198.3	116.1	55.3	40.9	24.3	13.7	8.8	6.3	0.78	0.52	0.18	0.14
0.25E-08	0.002830	360.8	198.8	116.9	56.3	45.1	28.6	15.7	10.4	7.6	0.89	0.60	0.21	0.17
0.50E-08	0.005659	361.0	199.5	118.2	57.8	52.0	35.6	19.1	13.0	9.8	1.07	0.73	0.26	0.21
0.10E-07	0.011312	361.5	201.1	120.8	60.9	65.8	49.7	25.8	18.2	14.2	1.44	0.98	0.37	0.29
0.25E-07	0.028240	362.8	205.6	128.5	70.2	106.4	91.1	45.9	33.8	27.3	2.51	1.75	0.67	0.54
0.50E-07	0.056346	365.0	213.0	141.2	85.6	171.8	158.0	78.8	59.3	48.9	4.29	3.00	1.18	0.96
0.10E-06	0.112164	369.1	227.5	166.0	115.6	295.2	284.3	142.8	109.0	90.9	7.77	5.46	2.17	1.77
0.25E-06	0.276816	378.8	265.6	233.0	198.4	604.3	601.3	318.8	246.3	208.2	17.71	12.51	5.02	4.10
0.50E-06	0.543087	389.0	318.2	329.7	321.5	981.8	990.4	574.2	446.8	382.2	32.91	23.29	9.42	7.73
0.10E-05	1.051946	394.3	393.2	480.6	525.4	1422.0	1446.6	982.1	771.7	673.7	60.11	42.62	17.40	14.34
0.20E-05	2.005341	372.6	468.8	673.8	827.0	1751.0	1786.1	1550.6	1239.0	1121.0	107.34	76.27	31.46	26.06
0.40E-05	3.758634	295.4	491.0	848.8	1213.7	1836.3	1851.6	2228.2	1833.8	1759.0	190.69	135.80	56.59	47.11
0.60E-05	5.383984	223.7	454.5	899.9	1456.2	1793.6	1776.3	2640.5	2229.2	2238.5	268.86	191.76	80.32	67.03
0.10E-04	8.390248	127.2	355.0	873.1	1737.2	1689.2	1616.5	3147.1	2769.9	2976.4	420.18	300.30	126.49	105.83
0.20E-04	15.035424	36.6	183.9	672.7	1967.0	1486.3	1350.5	3751.7	3547.7	4226.4	782.51	561.33	237.95	199.58

Table A.25. ASTRO-F fluxes for a O-rich AGB star, $T_{\text{eff}} = 3297$ K, 100% Silicate.

\dot{M}	τ	IRC_N2	IRC_N3	IRC_N4	S7	S9W	S11	L15	L18W	L24	N60	WIDE-S	WIDE-L	N160
0.10E-09	0.000134	525.0	294.4	185.1	89.3	63.2	36.2	21.0	13.3	9.4	1.23	0.82	0.28	0.22
0.25E-09	0.000334	525.0	294.4	185.1	89.4	63.6	36.6	21.2	13.5	9.5	1.24	0.82	0.28	0.22
0.50E-09	0.000668	525.0	294.5	185.2	89.5	64.2	37.2	21.5	13.7	9.7	1.26	0.84	0.29	0.23
0.10E-08	0.001337	525.0	294.6	185.4	89.8	65.3	38.3	22.1	14.1	10.0	1.29	0.86	0.30	0.23
0.25E-08	0.003342	525.0	294.9	186.1	90.6	68.8	41.9	23.8	15.5	11.2	1.38	0.92	0.32	0.26
0.50E-08	0.006681	524.9	295.4	187.1	91.9	74.6	47.8	26.6	17.7	13.0	1.53	1.03	0.37	0.29
0.10E-07	0.013355	524.8	296.5	189.2	94.5	86.2	59.6	32.3	22.1	16.7	1.84	1.25	0.45	0.36
0.25E-07	0.033331	524.4	299.7	195.4	102.3	120.3	94.5	49.3	35.3	27.9	2.76	1.90	0.71	0.57
0.50E-07	0.066475	523.7	305.0	205.7	115.2	175.5	151.0	77.3	57.1	46.3	4.29	2.98	1.15	0.93
0.10E-06	0.132220	522.2	315.3	226.0	140.7	280.1	258.1	132.5	99.9	82.6	7.31	5.12	2.01	1.63
0.25E-06	0.325542	517.3	343.1	282.0	212.9	544.3	529.6	287.1	220.7	186.1	16.14	11.36	4.52	3.69
0.50E-06	0.636353	507.4	382.9	366.3	324.8	876.5	872.6	520.5	404.3	346.3	30.23	21.35	8.58	7.02
0.10E-05	1.224941	482.9	440.7	503.4	519.2	1283.4	1294.6	910.1	715.5	626.9	56.57	40.04	16.23	13.33
0.20E-05	2.312776	425.2	499.0	688.8	822.4	1628.1	1648.1	1479.5	1184.1	1076.5	104.08	73.84	30.23	24.96
0.40E-05	4.274016	314.4	505.5	862.2	1223.4	1771.3	1769.0	2175.0	1793.6	1728.3	188.84	134.28	55.56	46.11
0.60E-05	6.058981	229.2	461.1	911.5	1474.1	1759.3	1723.9	2597.8	2197.3	2214.8	267.92	190.79	79.41	66.09
0.10E-04	9.300130	125.2	354.4	879.2	1757.6	1677.3	1588.7	3114.1	2745.2	2957.6	420.17	299.88	125.66	104.89
0.20E-04	16.298681	35.0	181.1	670.9	1975.7	1483.5	1340.1	3730.8	3531.2	4211.3	783.07	561.16	237.01	198.48

Table A.26. ASTRO-F fluxes for a O-rich AGB star, $T_{\text{eff}} = 2500$ K, 100% Silicate.

\dot{M}	τ	IRC_N2	IRC_N3	IRC_N4	S7	S9W	S11	L15	L18W	L24	N60	WIDE-S	WIDE-L	N160
0.10E-09	0.000144	667.9	458.3	362.0	198.2	144.0	86.5	54.8	35.0	24.8	3.34	2.22	0.77	0.60
0.25E-09	0.000361	667.9	458.3	362.1	198.3	144.3	86.8	55.0	35.1	24.9	3.35	2.22	0.77	0.60
0.50E-09	0.000722	667.9	458.4	362.1	198.4	144.8	87.3	55.3	35.3	25.1	3.36	2.23	0.77	0.61
0.10E-08	0.001445	667.8	458.4	362.3	198.6	145.8	88.4	55.8	35.7	25.4	3.39	2.25	0.78	0.61
0.25E-08	0.003611	667.6	458.6	362.8	199.3	149.0	91.6	57.3	36.9	26.4	3.47	2.31	0.81	0.63
0.50E-08	0.007219	667.4	459.0	363.7	200.4	154.2	96.9	59.9	38.9	28.1	3.62	2.41	0.85	0.67
0.10E-07	0.014430	666.8	459.6	365.3	202.7	164.5	107.5	65.1	42.9	31.5	3.90	2.61	0.93	0.73
0.25E-07	0.036011	665.1	461.6	370.3	209.6	195.1	138.9	80.5	55.0	41.7	4.75	3.21	1.17	0.93
0.50E-07	0.071808	662.3	464.9	378.6	221.0	244.5	189.6	106.1	74.9	58.6	6.16	4.21	1.57	1.26
0.10E-06	0.142781	656.7	471.3	394.9	243.6	338.4	286.0	156.6	114.3	92.1	8.97	6.20	2.37	1.91
0.25E-06	0.351215	640.7	488.6	440.8	308.4	575.9	531.0	299.4	226.2	188.4	17.25	12.06	4.73	3.84
0.50E-06	0.685568	615.0	513.4	510.6	410.3	876.5	842.5	517.9	398.7	339.7	30.67	21.58	8.58	7.01
0.10E-05	1.316403	566.1	547.8	625.5	590.7	1249.9	1231.5	888.9	696.1	609.3	56.21	39.70	15.98	13.10
0.20E-05	2.475791	477.1	574.2	781.0	877.4	1578.4	1570.0	1441.8	1152.9	1050.1	103.19	73.11	29.78	24.54
0.40E-05	4.548722	335.6	545.1	919.6	1262.5	1735.1	1708.5	2133.7	1761.1	1701.9	188.36	133.81	55.15	45.69
0.60E-05	6.420008	237.9	482.6	949.2	1505.2	1738.3	1683.0	2563.4	2171.2	2194.7	268.36	190.97	79.22	65.82
0.10E-04	9.786523	125.8	360.5	896.4	1779.6	1673.5	1572.2	3096.2	2732.6	2949.1	422.00	301.00	125.77	104.85
0.20E-04	16.987080	34.3	180.4	673.5	1987.8	1485.7	1337.2	3731.9	3535.2	4220.3	788.45	564.80	238.13	199.25

Table A.27. Optical, NIR, IRAC and MIPS magnitudes and fluxes for a C-rich post-AGB star, $T_{\text{eff}} = 2650$ K, 100% AMC.

T_c	τ	V	I	J	H	K	3.6	4.5	5.8	8.0	24	70	160
0.12E+04	1.046662	42.61	31.70	21.35	15.91	12.05	329.8	871.1	1599.8	2429.9	1568.50	372.92	134.401
0.11E+04	0.903924	38.97	29.06	20.22	15.38	11.83	344.1	886.1	1601.1	2420.3	1547.85	371.27	134.476
0.10E+04	0.763922	35.32	26.32	18.71	14.58	11.50	360.1	899.1	1595.3	2405.1	1530.56	371.33	135.275
0.90E+03	0.628735	31.73	23.65	17.08	13.59	11.07	375.2	905.4	1577.7	2384.3	1519.30	373.95	137.131
0.80E+03	0.496372	28.15	21.01	15.42	12.48	10.50	389.2	902.4	1543.5	2349.8	1507.28	377.22	139.409
0.70E+03	0.373292	24.74	18.55	13.86	11.39	9.87	388.1	868.4	1472.2	2295.2	1506.54	384.40	143.332
0.60E+03	0.264308	21.65	16.36	12.47	10.39	9.24	352.6	765.6	1318.2	2187.6	1545.88	405.25	152.731
0.50E+03	0.172424	18.99	14.50	11.29	9.54	8.66	288.0	576.7	1027.4	1930.1	1635.36	449.89	172.053
0.40E+03	0.100233	16.86	13.04	10.36	8.86	8.17	237.5	356.9	608.9	1391.1	1725.47	523.16	204.977
0.30E+03	0.048687	15.32	11.99	9.70	8.38	7.82	240.0	234.3	251.4	636.3	1624.21	598.06	244.832
0.20E+03	0.017105	14.37	11.34	9.29	8.08	7.60	265.0	225.7	139.6	133.1	1039.68	602.82	271.067
0.15E+03	0.008127	14.09	11.16	9.17	8.00	7.54	274.3	231.5	137.9	74.1	544.51	527.15	263.163
0.10E+03	0.002898	13.93	11.05	9.10	7.95	7.51	279.1	234.5	139.1	68.7	143.33	376.93	236.780
0.75E+02	0.001407	13.89	11.02	9.08	7.94	7.50	280.7	235.6	139.6	68.9	46.95	245.52	200.234
0.50E+02	0.000513	13.86	11.00	9.07	7.93	7.49	281.6	236.1	139.8	69.0	24.19	101.39	144.123
0.25E+02	0.000092	13.85	10.99	9.07	7.92	7.49	282.0	236.4	139.9	69.0	23.32	7.58	42.638
0.15E+02	0.000026	13.85	10.99	9.07	7.92	7.49	282.1	236.4	139.9	69.0	23.32	2.97	6.836
0.10E+02	0.000009	13.85	10.99	9.07	7.92	7.49	282.1	236.4	139.9	69.0	23.32	2.90	1.088

Table A.28. Optical, NIR, IRAC and MIPS magnitudes and fluxes for a C-rich post-AGB star, $T_{\text{eff}} = 3600$ K, 100% AMC.

M	τ	V	I	J	H	K	3.6	4.5	5.8	8.0	24	70	160
0.12E+04	0.980290	39.63	30.04	20.91	15.76	11.98	339.3	880.1	1607.4	2435.2	1549.74	370.21	133.849
0.11E+04	0.839955	35.97	27.32	19.62	15.18	11.76	355.3	893.8	1606.3	2424.3	1529.45	369.09	134.146
0.10E+04	0.702712	32.30	24.61	18.04	14.36	11.44	373.8	904.9	1597.5	2406.7	1512.62	369.83	135.247
0.90E+03	0.570039	28.68	21.97	16.41	13.37	11.02	394.5	912.1	1579.2	2381.3	1495.84	371.46	136.809
0.80E+03	0.445435	25.20	19.47	14.83	12.33	10.54	409.4	904.1	1542.9	2348.4	1486.45	375.95	139.613
0.70E+03	0.331322	21.94	17.17	13.37	11.31	10.01	406.9	864.1	1473.9	2301.8	1488.51	383.98	143.922
0.60E+03	0.232149	19.04	15.16	12.09	10.40	9.48	364.6	751.6	1326.4	2215.1	1535.93	406.23	153.864
0.50E+03	0.150163	16.59	13.49	11.03	9.63	8.98	286.6	545.0	1038.8	1989.1	1651.51	456.73	175.354
0.40E+03	0.086782	14.67	12.19	10.21	9.03	8.56	220.3	299.6	608.8	1469.8	1794.92	545.88	214.390
0.30E+03	0.042011	13.30	11.27	9.63	8.61	8.26	210.6	152.9	224.5	687.2	1755.17	648.98	265.941
0.20E+03	0.014737	12.46	10.71	9.27	8.35	8.07	228.5	132.3	96.8	135.0	1158.61	679.16	305.419
0.15E+03	0.007000	12.22	10.55	9.17	8.28	8.02	235.6	135.1	93.3	67.7	606.03	601.76	300.483
0.10E+03	0.002496	12.08	10.46	9.11	8.24	7.99	239.2	136.6	93.8	61.4	147.21	433.09	272.388
0.75E+02	0.001212	12.04	10.43	9.10	8.22	7.98	240.4	137.1	94.1	61.5	35.87	281.97	230.795
0.50E+02	0.000442	12.02	10.42	9.09	8.22	7.97	241.1	137.4	94.3	61.6	9.50	115.16	166.022
0.25E+02	0.000079	12.01	10.41	9.08	8.21	7.97	241.4	137.5	94.3	61.6	8.49	6.39	48.356
0.15E+02	0.000022	12.01	10.41	9.08	8.21	7.97	241.5	137.5	94.4	61.6	8.49	1.07	6.990
0.10E+02	0.000008	12.01	10.41	9.08	8.21	7.97	241.5	137.5	94.4	61.6	8.49	0.99	0.564

Table A.29. Optical, NIR, IRAC and MIPS magnitudes and fluxes for a O-rich post-AGB star, $T_{\text{eff}} = 3850$ K, 100% Silicate.

T_c	τ	V	I	J	H	K	3.6	4.5	5.8	8.0	24	70	160
0.10E+04	15.022061	33.24	24.39	17.93	14.42	11.70	291.9	695.8	1249.6	1717.1	4205.81	675.25	224.784
0.90E+03	12.476484	29.83	22.04	16.50	13.56	11.40	290.4	678.1	1212.6	1692.6	4243.28	675.71	227.586
0.80E+03	10.099082	26.58	19.81	15.10	12.62	11.01	279.9	641.3	1149.2	1656.0	4313.57	678.77	231.449
0.70E+03	7.949813	23.57	17.79	13.83	11.72	10.56	250.3	566.7	1036.3	1595.3	4439.93	685.39	236.700
0.60E+03	6.077328	20.89	16.02	12.72	10.90	10.07	198.4	439.9	846.2	1477.4	4639.07	699.86	245.028
0.50E+03	4.486949	18.58	14.50	11.77	10.20	9.58	142.3	277.8	577.4	1248.2	4865.82	724.29	257.750
0.40E+03	3.125848	16.57	13.20	10.96	9.60	9.14	114.2	141.7	295.8	878.4	4966.26	754.68	274.670
0.30E+03	1.907103	14.75	12.03	10.23	9.06	8.72	124.1	84.6	112.0	434.5	4664.11	783.65	295.822
0.20E+03	0.816058	13.09	10.98	9.58	8.57	8.36	151.3	86.7	65.1	107.0	3407.26	801.30	326.351
0.15E+03	0.394623	12.45	10.57	9.32	8.39	8.21	164.1	92.4	66.3	49.1	2112.86	777.22	342.699
0.10E+03	0.126920	12.04	10.31	9.16	8.27	8.12	172.8	96.2	68.5	41.4	621.41	640.40	337.303
0.75E+02	0.053711	11.92	10.24	9.12	8.23	8.10	175.4	97.4	69.2	41.7	150.92	467.08	306.863
0.50E+02	0.015665	11.86	10.20	9.09	8.22	8.08	176.8	98.1	69.6	42.0	11.04	200.11	227.046
0.25E+02	0.002210	11.84	10.19	9.09	8.21	8.08	177.3	98.3	69.7	42.1	5.29	10.56	69.881
0.15E+02	0.000574	11.84	10.19	9.08	8.21	8.08	177.3	98.3	69.7	42.1	5.29	0.76	10.637
0.10E+02	0.000196	11.84	10.19	9.08	8.21	8.08	177.3	98.3	69.7	42.1	5.29	0.61	0.739

Table A.30. Optical, NIR, IRAC and MIPS magnitudes and fluxes for a O-rich post-AGB star, $T_{\text{eff}} = 3297$ K, 100% Silicate.

T_c	τ	V	I	J	H	K	3.6	4.5	5.8	8.0	24	70	160
0.10E+04	16.290331	37.43	26.26	18.42	14.58	11.74	289.7	695.2	1255.3	1719.6	4193.92	678.37	224.747
0.90E+03	13.652185	34.02	23.87	16.97	13.71	11.42	288.9	678.8	1221.4	1698.2	4221.60	675.79	226.391
0.80E+03	11.150371	30.67	21.56	15.51	12.73	10.98	281.5	645.2	1163.3	1663.5	4282.63	678.58	230.116
0.70E+03	8.841756	27.48	19.42	14.14	11.75	10.44	258.6	575.9	1055.5	1601.6	4394.52	684.52	235.105
0.60E+03	6.794093	24.57	17.52	12.93	10.86	9.87	217.1	455.6	868.9	1478.3	4572.09	697.31	242.847
0.50E+03	5.037727	22.01	15.87	11.89	10.08	9.31	173.5	299.9	600.9	1240.6	4767.33	718.30	254.375
0.40E+03	3.533377	19.76	14.46	10.99	9.42	8.81	159.5	170.3	319.5	864.0	4816.21	741.63	268.796
0.30E+03	2.184232	17.71	13.19	10.19	8.82	8.36	186.1	121.9	140.4	425.4	4424.23	754.38	283.947
0.20E+03	0.953169	15.80	12.02	9.45	8.27	7.94	234.0	134.2	101.4	120.9	3078.80	733.84	298.710
0.15E+03	0.464518	15.04	11.55	9.16	8.06	7.78	256.8	144.5	105.6	72.2	1853.33	686.75	303.060
0.10E+03	0.149931	14.55	11.25	8.97	7.92	7.67	272.8	151.7	109.8	67.2	535.37	549.86	290.025
0.75E+02	0.063485	14.41	11.17	8.92	7.88	7.64	277.5	153.8	111.1	68.1	132.69	398.00	261.787
0.50E+02	0.018519	14.34	11.12	8.89	7.86	7.63	280.1	155.0	111.8	68.6	13.91	170.16	193.027
0.25E+02	0.002612	14.31	11.11	8.88	7.85	7.62	281.0	155.4	112.0	68.8	9.05	9.51	59.746
0.15E+02	0.000678	14.31	11.11	8.88	7.85	7.62	281.1	155.4	112.0	68.8	9.06	1.18	9.461
0.10E+02	0.000231	14.31	11.11	8.88	7.85	7.62	281.1	155.4	112.0	68.8	9.06	1.05	0.843

Table A.31. Optical, NIR, IRAC and MIPS magnitudes and fluxes for a O-rich post-AGB star, $T_{\text{eff}} = 2500$ K, 100% Silicate.

T_c	τ	V	I	J	H	K	3.6	4.5	5.8	8.0	24	70	160
0.10E+04	16.987080	40.68	28.28	18.62	14.79	11.79	289.4	698.3	1264.4	1726.4	4206.51	685.39	226.565
0.90E+03	14.282159	37.29	25.88	17.13	13.95	11.46	291.0	685.1	1232.9	1705.2	4221.75	679.07	226.872
0.80E+03	11.712989	33.95	23.54	15.63	12.96	10.99	288.7	657.6	1179.7	1669.2	4270.69	680.71	230.207
0.70E+03	9.322069	30.75	21.35	14.22	11.95	10.42	275.9	599.1	1080.0	1604.8	4362.60	684.98	234.649
0.60E+03	7.182675	27.78	19.39	12.95	11.03	9.80	250.5	496.1	906.6	1479.8	4509.55	694.86	241.422
0.50E+03	5.337032	25.14	17.69	11.86	10.22	9.22	227.6	362.4	656.7	1245.8	4666.47	711.31	251.375
0.40E+03	3.754286	22.80	16.22	10.92	9.52	8.70	237.0	256.4	395.9	881.5	4676.07	728.42	263.522
0.30E+03	2.334116	20.66	14.90	10.07	8.90	8.22	290.3	232.4	237.9	465.5	4252.73	732.20	275.160
0.20E+03	1.028638	18.65	13.68	9.29	8.32	7.78	370.9	271.4	219.2	188.0	2913.59	698.16	283.880
0.15E+03	0.503405	17.83	13.19	8.98	8.09	7.61	409.8	294.0	232.0	148.9	1741.36	644.70	284.284
0.10E+03	0.162798	17.30	12.87	8.77	7.94	7.49	437.3	309.8	242.1	149.0	509.78	510.81	269.129
0.75E+02	0.068956	17.15	12.78	8.71	7.90	7.46	445.5	314.5	245.2	151.2	137.87	369.12	242.223
0.50E+02	0.020116	17.07	12.74	8.68	7.88	7.44	449.9	317.1	246.9	152.4	28.53	158.66	178.472
0.25E+02	0.002838	17.04	12.72	8.67	7.87	7.44	451.3	317.9	247.4	152.8	24.10	10.65	55.653
0.15E+02	0.000737	17.04	12.72	8.67	7.87	7.44	451.5	318.0	247.5	152.9	24.11	2.97	9.301
0.10E+02	0.000251	17.04	12.72	8.67	7.87	7.44	451.6	318.0	247.5	152.9	24.11	2.85	1.277

Table A.32. ASTRO-F fluxes for a C-rich post-AGB star, $T_{\text{eff}} = 2650$ K, 100% AMC.

T_c	τ	IRC_N2	IRC_N3	IRC_N4	S7	S9W	S11	L15	L18W	L24	N60	WIDE-S	WIDE-L	N160
0.12E+04	1.046662	33.8	200.9	835.1	2475.2	2863.3	2473.0	2368.5	1754.2	1588.1	417.23	318.25	142.47	117.77
0.11E+04	0.903924	38.3	211.6	850.2	2468.3	2842.6	2446.5	2331.5	1728.1	1567.0	415.12	317.18	142.46	117.90
0.10E+04	0.763922	45.4	224.1	863.9	2454.4	2816.5	2416.9	2295.3	1703.8	1549.3	414.86	317.64	143.21	118.66
0.90E+03	0.628735	56.5	237.2	871.3	2432.2	2785.9	2386.2	2262.6	1683.8	1537.6	417.38	320.38	145.08	120.35
0.80E+03	0.496372	76.1	251.4	870.4	2393.6	2741.1	2345.6	2224.5	1661.0	1525.0	420.56	323.82	147.39	122.41
0.70E+03	0.373292	108.6	258.0	839.7	2326.5	2681.9	2302.2	2195.3	1647.4	1523.7	428.02	330.72	151.42	125.92
0.60E+03	0.264308	160.9	246.4	742.7	2187.5	2587.5	2256.6	2201.8	1667.9	1562.5	450.56	349.61	161.21	134.26
0.50E+03	0.172424	243.4	223.4	564.6	1875.7	2361.5	2144.1	2224.6	1718.4	1651.0	499.14	389.56	181.38	151.36
0.40E+03	0.100233	357.5	217.4	359.8	1285.1	1832.5	1803.3	2139.1	1720.5	1737.6	578.30	455.79	215.65	180.54
0.30E+03	0.048687	479.6	243.6	248.2	548.7	965.1	1090.8	1680.6	1466.1	1627.4	656.58	526.83	256.60	216.16
0.20E+03	0.017105	576.1	275.6	242.8	130.3	220.6	287.8	728.2	765.5	1029.7	651.55	544.15	281.81	240.54
0.15E+03	0.008127	608.4	286.6	249.3	92.0	86.8	86.3	263.1	334.6	532.6	559.33	490.09	271.37	234.73
0.10E+03	0.002898	626.5	292.5	252.8	89.7	65.7	40.9	50.1	73.7	137.4	384.26	375.51	240.05	213.42
0.75E+02	0.001407	632.2	294.4	254.0	90.0	65.5	39.4	27.6	29.3	45.3	239.68	265.69	199.13	182.60
0.50E+02	0.000513	635.4	295.4	254.6	90.1	65.5	39.3	25.2	21.3	24.4	90.75	132.12	137.62	134.70
0.25E+02	0.000092	637.0	296.0	255.0	90.2	65.6	39.4	25.2	21.0	23.6	6.40	14.33	36.50	42.70
0.15E+02	0.000026	637.3	296.0	255.0	90.2	65.6	39.4	25.2	21.0	23.6	3.41	2.67	5.54	7.24
0.10E+02	0.000009	637.3	296.1	255.0	90.2	65.6	39.4	25.2	21.0	23.6	3.39	2.26	1.06	1.03

Table A.33. ASTRO-F fluxes for a C-rich post-AGB star, $T_{\text{eff}} = 3600$ K, 100% AMC.

T_c	τ	IRC_N2	IRC_N3	IRC_N4	S7	S9W	S11	L15	L18W	L24	N60	WIDE-S	WIDE-L	N160
0.12E+04	0.980290	35.5	208.1	844.7	2483.2	2862.8	2466.3	2352.1	1738.7	1569.2	414.03	316.18	141.83	117.33
0.11E+04	0.839955	40.3	220.4	859.0	2474.7	2840.4	2438.3	2314.6	1712.5	1548.5	412.49	315.58	142.06	117.65
0.10E+04	0.702712	47.7	235.6	871.4	2458.3	2811.3	2406.4	2277.7	1688.1	1531.2	412.95	316.67	143.14	118.68
0.90E+03	0.570039	59.0	253.7	880.7	2432.6	2773.3	2367.6	2236.7	1661.9	1513.8	414.34	318.62	144.69	120.11
0.80E+03	0.445435	75.1	269.7	875.5	2395.3	2730.1	2328.5	2201.3	1641.5	1503.9	418.85	323.16	147.55	122.63
0.70E+03	0.331322	98.2	276.1	839.2	2336.6	2679.2	2291.4	2177.1	1631.3	1505.4	427.23	330.83	151.99	126.48
0.60E+03	0.232149	130.4	259.5	732.7	2218.1	2608.7	2265.6	2199.4	1662.4	1552.4	451.35	350.92	162.34	135.29
0.50E+03	0.150163	178.8	226.1	536.8	1933.9	2424.0	2192.9	2262.3	1742.6	1667.3	506.52	395.88	184.80	154.30
0.40E+03	0.086782	245.6	207.2	306.7	1354.9	1931.6	1897.8	2241.7	1797.5	1807.6	603.29	475.86	225.51	188.87
0.30E+03	0.042011	316.4	222.5	171.2	585.6	1045.7	1186.3	1828.2	1590.2	1758.6	712.40	571.87	278.72	234.80
0.20E+03	0.014737	370.8	246.9	153.7	124.8	233.3	315.4	815.7	855.1	1147.3	733.90	613.27	317.59	270.99
0.15E+03	0.007000	389.0	255.6	157.2	80.8	81.5	87.4	292.5	372.0	592.3	638.26	559.77	309.94	267.96
0.10E+03	0.002496	398.8	260.0	159.0	77.9	57.1	35.3	48.5	73.4	140.2	441.18	431.96	276.23	245.45
0.75E+02	0.001212	402.0	261.5	159.7	78.1	56.8	33.5	22.4	22.0	33.8	274.81	305.84	229.57	210.42
0.50E+02	0.000442	403.7	262.3	160.0	78.2	56.8	33.4	19.7	12.7	9.5	102.43	151.32	158.54	155.15
0.25E+02	0.000079	404.6	262.7	160.2	78.2	56.9	33.5	19.7	12.4	8.7	4.63	14.73	41.29	48.48
0.15E+02	0.000022	404.7	262.7	160.2	78.2	56.9	33.5	19.7	12.4	8.7	1.19	1.24	5.51	7.51
0.10E+02	0.000008	404.8	262.8	160.2	78.2	56.9	33.5	19.7	12.4	8.7	1.16	0.77	0.51	0.58

Table A.34. ASTRO-F fluxes for a O-rich post-AGB star, $T_{\text{eff}} = 3850$ K, 100% Silicate.

T_c	τ	IRC_N2	IRC_N3	IRC_N4	S7	S9W	S11	L15	L18W	L24	N60	WIDE-S	WIDE-L	N160
0.10E+04	15.022061	36.4	183.4	671.0	1962.5	1494.7	1364.0	3761.2	3551.3	4221.2	776.60	556.97	235.97	197.87
0.90E+03	12.476484	41.3	184.8	655.0	1913.1	1490.7	1389.8	3814.2	3593.5	4260.0	776.43	558.33	238.47	200.63
0.80E+03	10.099082	48.3	181.1	620.4	1834.8	1489.2	1438.1	3909.7	3671.5	4332.7	779.07	562.07	242.10	204.31
0.70E+03	7.949813	58.3	166.1	549.3	1703.1	1499.1	1534.9	4080.8	3813.9	4463.9	785.59	568.99	247.21	209.19
0.60E+03	6.077328	74.3	139.0	428.1	1478.3	1516.9	1691.9	4330.6	4033.0	4670.9	800.82	582.76	255.55	216.78
0.50E+03	4.486949	102.2	113.6	274.4	1125.6	1509.2	1865.4	4560.9	4265.5	4907.1	826.85	605.42	268.44	228.26
0.40E+03	3.125848	145.9	110.0	147.3	676.5	1399.4	1908.2	4524.3	4323.7	5013.8	858.44	634.31	285.55	243.52
0.30E+03	1.907103	206.8	131.9	96.1	269.5	1068.2	1566.5	3853.5	3895.3	4705.3	885.84	664.62	306.69	262.72
0.20E+03	0.816058	283.8	165.9	101.3	72.4	417.6	640.3	2130.7	2494.0	3414.3	893.52	692.54	336.33	290.89
0.15E+03	0.394623	320.9	181.6	108.3	54.2	125.3	183.7	955.3	1327.5	2094.5	853.48	685.77	351.06	306.60
0.10E+03	0.126920	346.9	192.4	113.1	53.9	39.2	27.5	152.6	298.8	600.1	678.96	594.42	341.31	304.06
0.75E+02	0.053711	354.7	195.6	114.5	54.3	37.5	21.1	29.7	63.0	141.8	475.42	463.65	305.88	279.13
0.50E+02	0.015665	358.9	197.4	115.3	54.6	37.9	21.3	12.5	9.4	10.4	185.80	236.99	217.85	211.30
0.25E+02	0.002210	360.3	197.9	115.6	54.7	38.1	21.5	12.3	7.8	5.4	7.50	23.24	59.89	69.76
0.15E+02	0.000574	360.5	198.0	115.6	54.7	38.1	21.5	12.3	7.8	5.4	0.77	1.26	8.33	11.44
0.10E+02	0.000196	360.5	198.0	115.6	54.7	38.2	21.5	12.3	7.8	5.4	0.71	0.48	0.60	0.82

Table A.35. ASTRO-F fluxes for a O-rich post-AGB star, $T_{\text{eff}} = 3297$ K, 100% Silicate.

T_c	τ	IRC_N2	IRC_N3	IRC_N4	S7	S9W	S11	L15	L18W	L24	N60	WIDE-S	WIDE-L	N160
0.10E+04	16.290331	34.9	181.0	670.4	1973.8	1487.0	1345.6	3734.3	3532.2	4208.4	780.38	559.18	236.12	197.71
0.90E+03	13.652185	39.6	182.6	655.7	1928.9	1487.2	1373.7	3782.9	3568.7	4237.5	776.84	557.94	237.41	199.44
0.80E+03	11.150371	47.6	180.9	624.7	1858.1	1482.8	1412.8	3863.5	3634.9	4300.5	779.24	561.36	240.88	203.01
0.70E+03	8.841756	61.1	171.1	559.5	1732.1	1483.4	1492.1	4010.8	3758.2	4416.4	785.04	567.63	245.70	207.68
0.60E+03	6.794093	84.7	152.6	446.0	1508.7	1481.6	1621.1	4228.5	3950.6	4600.7	798.37	579.96	253.42	214.76
0.50E+03	5.037727	125.3	138.0	300.2	1151.6	1442.1	1756.5	4420.8	4148.5	4804.3	820.46	599.75	265.05	225.20
0.40E+03	3.533377	188.2	147.2	181.2	695.2	1294.9	1757.9	4338.0	4159.6	4858.4	843.97	622.74	279.56	238.25
0.30E+03	2.184232	277.5	185.2	140.6	287.8	950.5	1401.0	3614.3	3665.7	4459.7	852.94	639.40	294.46	252.13
0.20E+03	0.953169	397.1	240.0	158.5	100.8	372.2	559.2	1911.5	2241.7	3083.2	818.25	634.16	307.86	266.25
0.15E+03	0.464518	457.8	266.2	171.4	86.4	130.7	169.5	840.1	1163.7	1836.7	754.07	605.97	310.40	271.18
0.10E+03	0.149931	501.8	284.7	180.3	87.7	62.0	39.4	140.0	261.4	517.2	582.97	510.37	293.37	261.52
0.75E+02	0.063485	515.1	290.2	183.0	88.6	61.6	34.9	35.5	60.1	125.1	405.16	394.99	260.85	238.21
0.50E+02	0.018519	522.2	293.2	184.5	89.1	62.6	35.6	21.0	14.6	13.5	158.12	201.31	185.14	179.70
0.25E+02	0.002612	524.7	294.2	185.0	89.2	63.0	35.9	20.9	13.2	9.3	7.00	20.14	51.20	59.66
0.15E+02	0.000678	525.0	294.3	185.0	89.2	63.0	35.9	20.9	13.3	9.3	1.28	1.50	7.44	10.16
0.10E+02	0.000231	525.0	294.4	185.0	89.3	63.0	36.0	20.9	13.3	9.3	1.23	0.82	0.72	0.91

Table A.36. ASTRO-F fluxes for a O-rich post-AGB star, $T_{\text{eff}} = 2500$ K, 100% Silicate.

T_c	τ	IRC_N2	IRC_N3	IRC_N4	S7	S9W	S11	L15	L18W	L24	N60	WIDE-S	WIDE-L	N160
0.10E+04	16.987080	34.3	180.4	673.5	1987.8	1485.7	1337.2	3731.9	3535.2	4220.3	788.45	564.80	238.13	199.25
0.90E+03	14.282159	39.5	183.7	662.1	1943.4	1488.5	1367.4	3774.9	3564.6	4237.3	780.69	560.43	238.03	199.79
0.80E+03	11.712989	49.0	186.3	637.5	1875.0	1480.6	1399.1	3840.6	3618.2	4287.9	781.80	562.87	241.08	203.02
0.70E+03	9.322069	66.3	184.8	584.0	1752.5	1473.0	1463.7	3962.1	3720.1	4383.2	785.69	567.74	245.32	207.22
0.60E+03	7.182675	97.2	180.0	488.8	1535.8	1457.8	1569.2	4142.5	3880.0	4536.0	795.69	577.64	252.00	213.45
0.50E+03	5.337032	149.4	183.8	366.2	1190.6	1402.8	1677.2	4295.1	4040.5	4700.4	812.58	593.64	261.98	222.50
0.40E+03	3.754286	228.9	214.9	272.7	751.0	1246.1	1659.5	4183.8	4018.9	4714.6	829.02	611.39	274.12	233.55
0.30E+03	2.334116	342.0	279.3	258.9	363.8	916.5	1315.4	3461.2	3511.2	4284.8	827.95	620.36	285.39	244.31
0.20E+03	1.028638	496.9	367.9	306.7	196.2	398.0	543.3	1819.3	2122.8	2917.0	778.54	603.15	292.60	253.02
0.15E+03	0.503405	577.4	411.2	333.4	188.8	190.4	195.3	811.8	1102.5	1725.8	708.01	568.71	291.17	254.38
0.10E+03	0.162798	636.6	442.1	352.2	194.4	137.4	84.5	163.3	263.1	493.3	541.76	473.87	272.22	242.69
0.75E+02	0.068956	654.5	451.4	357.8	196.5	140.1	83.1	67.6	77.7	131.2	376.04	365.94	241.36	220.42
0.50E+02	0.020116	664.1	456.3	360.8	197.7	142.7	85.3	54.7	36.0	28.5	147.88	186.94	171.21	166.15
0.25E+02	0.002838	667.4	458.0	361.8	198.1	143.6	86.1	54.7	34.9	24.7	8.66	20.03	47.79	55.52
0.15E+02	0.000737	667.8	458.2	361.9	198.1	143.7	86.2	54.7	34.9	24.7	3.38	2.85	7.45	9.89
0.10E+02	0.000251	667.9	458.3	362.0	198.1	143.7	86.2	54.7	34.9	24.7	3.33	2.22	1.19	1.27